Effetto pro-osteogenico sinergico di perfusione e stimolazione elettromagnetica pulsata su modelli biomimetici di tessuto osseo

processes

MDPI

Review

Removal of Agrochemicals from Waters by Adsorption: A Critical Comparison among Humic-Like Substances, Zeolites, Porous Oxides, and Magnetic Nanocomposites

Antonello Marocco [1], Gianfranco Dell'Agli [1], Filomena Sannino [2,*], Serena Esposito [3], Barbara Bonelli [3], Paolo Allia [3], Paola Tiberto [4], Gabriele Barrera [4] and Michele Pansini [1]

1 Department of Civil and Mechanical Engineering and INSTM Research Unit, Università degli Studi di Cassino e del Lazio Meridionale, Via G. Di Biasio 43, 03043 Cassino, FR, Italy; a.marocco@unicas.it (A.M.); dellagli@unicas.it (G.D.); pansini@unicas.it (M.P.)
2 Department of Agricultural Sciences, Università di Napoli "Federico II", Via Università 100, 80055 Portici, NA, Italy
3 Department of Applied Science and Technology and INSTM Unit of Torino-Politecnico, Politecnico di Torino, Corso Duca degli Abruzzi 24, 10129 Torino, Italy; serena_esposito@polito.it (S.E.); barbara.bonelli@polito.it (B.B.); paolo.allia@polito.it (P.A.)
4 INRIM, Nanoscience and Materials Division, Strada delle Cacce 91, 10135 Torino, Italy; p.tiberto@inrim.it (P.T.); g.barrera@inrim.it (G.B.)
* Correspondence: filomena.sannino@unina.it; Tel.: +39-0812539187

Received: 16 December 2019; Accepted: 16 January 2020; Published: 21 January 2020

Abstract: The use of humic-like substances, zeolites, various porous oxides (i.e., Al, Fe, or Si oxides), and magnetic nanocomposites in the adsorption of agrochemicals from water was critically reviewed. Firstly, the adsorbents were characterized from the structural, textural, and physico-chemical points of view. Secondly, the fundamental aspects of the adsorption of various agrochemicals on the solids (dependence on pH, kinetics, and isotherm of adsorption) were studied and interpreted on the basis of the adsorbent features. Thirdly, iterative processes of agrochemical removal from water by adsorption on the reported solids were described. In particular, in some cases the residual concentration of agrochemicals in water was lower than the maximum concentration of agrochemicals that the Italian regulations allow to be released in wastewater, surface waters, or sink water.

Keywords: adsorption; agrochemicals; humic-like substances; zeolites; porous oxides; magnetic nanocomposites

1. Introduction

The use of agrochemicals, although unpleasant, appears absolutely necessary to tackle the various kinds of adverse events that can largely damage the quality of the various crops, and allows for a significant increase in production. In association with this benefit, the risk of environmental pollution must be considered. Besides environmental pollution, the use of agrochemicals may give rise to many serious pathologies for human beings [1]. Besides the fact that the soil and the surface water are mostly exposed to them, the harmfulness of agrochemicals is enhanced by their mobility and persistence in the aqueous media [2] and by the fact that they can be dangerous also at low (sometimes not detectable) concentrations, which make them a type of emerging contaminants [3]. In order to protect the environment and human health it is important to develop proper methodologies to prevent water and/or soil contamination by agrochemicals and to remediate contaminated soils and water

bodies. The increasing concern towards agrochemicals is confirmed by many scientific works [1–19], which propose many different methods for their removal.

Among them, adsorption enjoys a large consideration owing to its efficiency, intrinsic simplicity, and low cost. In particular, activated carbons are the most widely used adsorbents for agrochemical removal from water [20–22]. Although activated carbons are among the most effective adsorbents owing to their high surface area, their use does not appear free from troubles. Actually, a considerable fraction of activated carbon is lost during each cycle of its regeneration, which is performed by thermal desorption or combustion, and the loss of adsorbent is a major economic consideration in any large-scale remediation application [21].

The above considerations worldwide promoted active research on the use of adsorbents (other than activated carbons) for agrochemical removal from water and the production of innovative and efficient adsorbents. This work intends to critically review the data regarding agrochemical adsorption on a selection of adsorbents, namely (1) a material of natural origin mainly formed by humic-like substances, (2) zeolites, and (3) various porous oxides (of Fe, Al or Si) and some magnetic metal-ceramic nanocomposites obtained through a simple and low-cost process based on the use of transition metal-exchanged commercial zeolites as a smart precursor. The reasons for the particular selection of adsorbents are the following:

1. Materials of natural origin mainly formed by humic-like substances are often by-products of many processes of the food industry. Such materials, which are wastes to be disposed of, exhibit some adsorption and cation exchange properties [23–26]. It would be extremely attractive to use such waste materials in the remediation of waters polluted by agrochemicals. Moreover, after adsorption, such natural materials can be easily composted, allowing the destruction of the adsorbed agrochemicals [27–29].
2. Zeolites characteristically exhibit adsorption and cation exchange properties [30,31]. Moreover, the cost of many commercial zeolites is very low on account of their widespread availability [32] and the fact that processes for their production were optimized a long ago [33]. Finally, the use of zeolites for environmental purposes is well established [34,35].
3. Oxides of various elements, with different degrees of porosity, are commercially available at low cost and/or may be produced by a number of techniques, such as sol-gel methods [36–39]. Such porous oxides are known to exhibit very good adsorption properties [40–43].
4. Adsorption processes from liquid phase are performed either by flowing the liquid phase through a fixed bed of adsorbing material in a columnar plant or by dispersing the adsorbent in the liquid phase in batch reactors. Both alternatives exhibit problems: columnar plants are subjected to channeling and head losses, which worsen the liquid–adsorbent contact and may complicate the control of the process itself, whereas the separation of the exhausted adsorbent from the liquid is the most prominent problem in batch reactors. The use of magnetic adsorbents would allow for performing the adsorption process in a batch reactor system, thus obtaining a very intimate liquid–adsorbent contact, but avoiding all the troubles related to the solid separation, by simply using an external magnet to separate the magnetic adsorbent from the liquid phase.

Data on agrochemical removal from waters by using the adsorbents reported in the works hereafter reviewed are used to study the features of the kinetics and equilibrium, which permits a better understanding of the various kind of interplays between the agrochemical molecules and the adsorbent active sites.

Moreover, the evolution of the logical set up of scientific works concerning agrochemicals removal from water will be shown. Actually, the reader will see how, in more recent works, together with the scientific speculations deriving from the traditional elaboration of adsorption data in terms of equilibrium and kinetic modelling, growing attention is being paid to the legal limits of agrochemicals in various types of water.

In this work, adsorption of the following agrochemicals is addressed: 2,4 dichlorophenoxyacetic acid (referred to as 2,4 D), 1,1′-dimethyl-4,4′-bipyridinium (referred to as paraquat), (R)-2-(4-(4-cyano-2-fluorophenoxy) phenoxy) propionic acid (referred to as cyhalofop), 4-chloro-2-methylphenoxyacetic acid (referred to as MCPA), and 2-chloro-4,6-bis (ethylamino)-s-triazine (referred to as simazine). The presence of such agrochemicals is very often detected in water bodies and soils as they have been largely used as pre-emergence control of broad-leaf weeds and annual grasses in agricultural and non-crop fields [44–46]. Their harmfulness and carcinogenic potential are well documented and are matters of increasing concern [47] because they can be dangerous at low (hardly detectable) concentrations [3].

2. Materials and Methods

2.1. Materials

2,4 Dichlorophenoxyacetic acid (2,4 D) was supplied either by GmbH (99.6% purity) [48] or by Sigma-Aldrich Chemical Company (99.0% purity) [46]; 1,1′-dimethyl-4,4′-bipyridinium (paraquat) was supplied by Sigma-Aldrich Chemical Company, St. Louis, MO, USA, (99.0% purity) [49]; (R)-2-(4-(4-cyano-2-fluorophenoxy) phenoxy) propionic acid (cyhalofop) was supplied by Dow Agroscience B. V. Rotterdam (99.0% purity) [50]; 4-chloro-2-methylphenoxyacetic acid (MCPA) was supplied by Sigma-Aldrich Chemical Company (99.0% purity) [21]; and 2-chloro-4,6-bis (ethylamino)-s-triazine (simazine) was supplied by Sigma-Aldrich Chemical Company (99.0% purity) [51–58]. Their structures are reported in Figure 1.

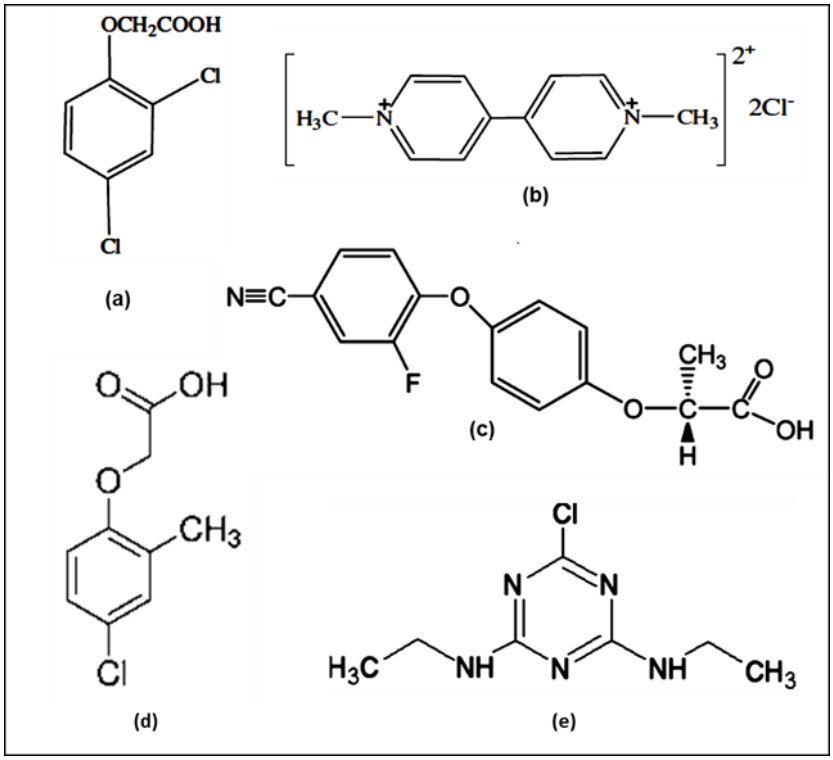

Figure 1. Structure formulas of the agrochemicals: (**a**) 2,4 dichlorophenoxyacetic acid (2,4-D); (**b**) 1,1′-dimethyl-4,4′-bipyridinium (paraquat); (**c**) (R)-2-(4-(4-cyano-2-fluorophenoxy) phenoxy) propionic acid (cyhalofop); (**d**) 4-chloro-2-methylphenoxyacetic acid (MCPA); (**e**) 2-chloro-4,6-bis (ethylamino)-s-triazine (simazine).

2.2. Methods

The methods and the procedures followed in the adsorption experiments were accurately described in [21,48–58].

The following experimental conditions were evaluated:

1. *pH*. The various adsorbents were contacted with an agrochemical solution of appropriate concentration at various solid/liquid ratios (s/l). The pH of the solution was properly varied by steps of 0.5, by addition of either 0.01 or 0.10 mmol/L HCl or NaOH solution. Each adsorption run lasted as long as necessary to reach equilibrium [21,48–58] and the pH of maximum adsorption for a given agrochemical/adsorbent system was determined at 25 °C.
2. *Adsorption time*. Kinetic studies were performed at the (previously determined) pH of maximum adsorption by contacting the selected adsorbent with the agrochemical solution of appropriate concentration at various contact times. The longest contact time was that needed to attain equilibrium [21,48–58].
3. *Adsorption isotherm*. Each adsorbent was contacted with solutions of appropriate agrochemical concentration, at selected s/l, at the (previously determined) pH of maximum adsorption at 25 °C. The pH of each suspension was kept constant by adding proper amounts of 0.01 or 0.10 mmol/LHCl or NaOH solution. The adsorption time of each run was selected so as to attain equilibrium [21,48–58].
4. *Solid/liquid ratio*. Adsorption runs were performed at various s/l ratios [21,48–58].

Iterative experiments of agrochemical removal from water were performed as follows. The selected adsorbent was contacted with an agrochemical aqueous solution at various s/l ratios and at the pH at which the maximum adsorption occurs, for a time sufficient to attain equilibrium. The selected initial agrochemical concentration was similar to that occurring in natural waters and water bodies [15,16]. Subsequently, solids were separated from liquids according to [21,48–58] and the equilibrium agrochemical concentration was determined. The same solution was newly contacted with fresh adsorbent at the same s/l ratio and the procedure was repeated until the equilibrium agrochemical concentration did not sensibly change [21,48–58]. X-ray diffraction (XRD) patterns were recorded according to the conditions reported in [59–61]. Diffuse reflectance infrared Fourier transform (DRIFT) spectra of selected adsorbents were obtained according to [21,48–58].

ζ-potential curves of selected adsorbents in deionized water were obtained and the point of zero charge (PZC) determined according to [21,48–58].

In some cases, the agrochemical was characterized by simultaneous differential thermal analysis (DTA) and thermogravimetric analysis (TG) according to [21,48–58].

Metal–ceramic nanocomposites were subjected to magnetic characterization according to [58].

3. Results and Discussion

3.1. Adsorption on Humic-Like Substances

The use of vegetal biomass with high sorption capacity to remediate waters that are polluted by agrochemicals was already described [62]. Among such vegetal biomasses, the use of the organic fraction of olive oil mill wastewater appears particularly interesting, as it is a cost-free agricultural waste, which would require disposal and possesses humic acid-like characteristics [63]. Such an organic fraction of olive oil mill wastewater assumes polymeric features and is, indeed, named polymerin [62]: it exhibits potential for the bioremediation of water contaminated with agrochemicals [63]. In particular, polymerin was subjected to both chemical and DRIFTS (Diffuse Reflectance Infrared Fourier Transform Spectroscopy) analysis, which confirmed that it is a humic-like polyelectrolyte consisting of carbohydrates, melanin, and proteins, naturally bounding some metals (Ca, Mg, K, Na, and Fe) that are chelated by carboxylate anions and/or other nucleophilic functional groups [63]. Moreover, the

point of zero charge of polymerin is 2.2, its negative charge increasing with the pH, and it has a pKa of 4.5, in agreement with the presence of mildly acidic carboxyl and phenolic groups.

Adsorption of paraquat, 2,4-D and cyhalofop [64] on polymerin was studied at various pH and s/l. In particular, 10, 25, and 50 mg of polymerin were added to 20 mL of water (s/l = 1/2000, 1/800, 1/400, respectively) bearing 0.27 and 0.22 mmol/L of paraquat and 2,4-D, respectively, and 10 mg of polymerin were added to 20 mL of water (s/l = 1/2000) [49,50]. As expected, both the residual agrochemical concentration in water and the amount of agrochemical adsorbed per gram of sorbent decreased with increasing s/l. Concerning the influence of pH, the maximum adsorbed amount of paraquat, 2,4-D and cyhalofop was obtained at pH 5.7, 2.0 and 4.5, respectively. Such findings were interpreted as follows. Paraquat is present in water either as a cation at acidic-neutral pH or as a neutral species at basic pHs. The maximum of interaction between paraquat and polymerin occurs at a pH = 5.7, i.e., when it occurs as a cation and the surface of polymeryn is covered by a sufficient number of negatively charged sites, which are the more numerous the higher the pH. Thus, adsorption of paraquat on polymerin is low both at acidic pH, on account of the low number of negatively charged sites at the surface of polymerin, and at basic pH, as paraquat loses its cationic character. Unlike paraquat, 2,4-D exhibits prevailingly anionic/non-ionic character and, thus, is adsorbed on polymerin through the formation of hydrogen bonds between the 2,4-D molecule and the humic acids of the solid surface. As expected, the formation of such hydrogen bonds occurs due to the lower pH and becomes appreciable only at pH $\leq$ 3 [49].

As far as cyhalofop adsorption on polymerin is concerned, this process could be probably ascribed to the formation of hydrogen bonds between the OH of the alcoholic groups of the polysaccharide component and the nitrile groups, and the undissociated carboxylic group of cyhalofop (pK_a = 3.8, [63]). Therefore, at pH = 4.5 the effect of hydrogen bonding is stronger than the repulsion between the ionized carboxylic group of polymerin and the agrochemical. On the contrary, a significant decrease in the adsorbed amount of cyhalofop was detected at pH > 4.5 as the agrochemical and polymerin carboxylic groups were mainly dissociated, with consequent dominant effect of repulsion [50].

Kinetics of adsorption of paraquat, 2,4-D and cyhalofop on polymerin, at the pHs of maximum adsorption, were also investigated. Adsorption of also paraquat was found to occur quickly (less than 2 h needed to attain equilibrium), unlike the adsorption of the other two agrochemicals (24 h to attain equilibrium). Such a large difference was explained as follows: both 2,4-D and cyhalofop were likely adsorb as undissociated species, in equilibrium with their anionic form. Removal of molecular 2,4-D and cyhalofop results in the conversion of the anionic forms into their molecular forms, thus giving rise to a much slower process. Such processes do not occur during paraquat adsorption on polymerin, where a mere electrostatic attraction occurs. Finally, adsorption of paraquat and cyhalofop on polymerin was found to be a pseudo-first order process, whereas no indication of the order of the kinetics was given for adsorption of 2,4-D [49,50].

Adsorption isotherms of paraquat, 2,4-D, and cyhalofop on polymerin, at the pH of maximum adsorption, are reported in Figures 2 and 3 [49,50], respectively. Adsorption of the agrochemicals increased slowly with equilibrium concentrations and satisfactory curve-fits were obtained by using the Langmuir equation [65]. Isothermal adsorption experiments were not performed so as to attain a plateau. Figures 2 and 3 indicate the highest agrochemical adsorbed amount at the relevant agrochemical concentration and s/l, which are reported in Table 1.

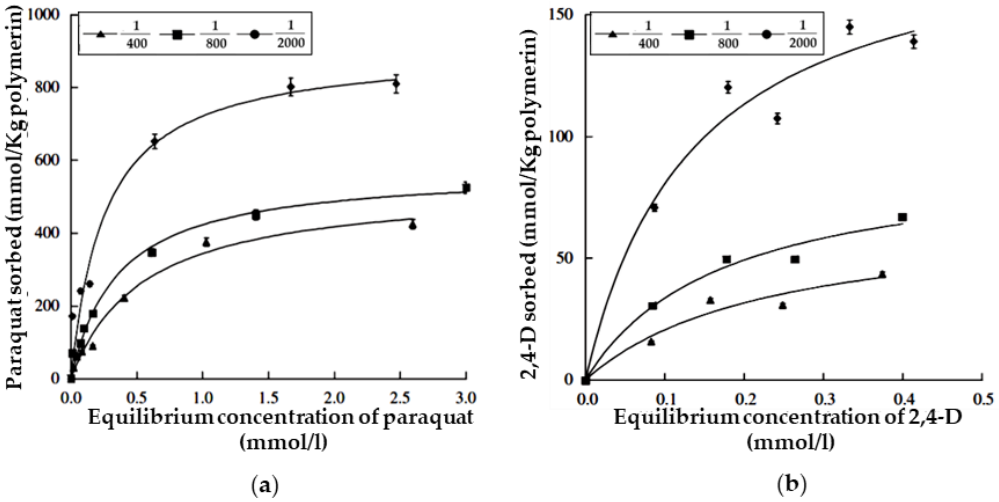

Figure 2. Adsorption isotherms of paraquat (**a**) or 2,4-D (**b**) on polymerin at solid/liquid ratios of 1/2000, 1/800, and 1/400 and at the pH of maximum adsorption. Reproduced with permission from Sannino et al., *Water Research*, published by Elsevier, 2008.

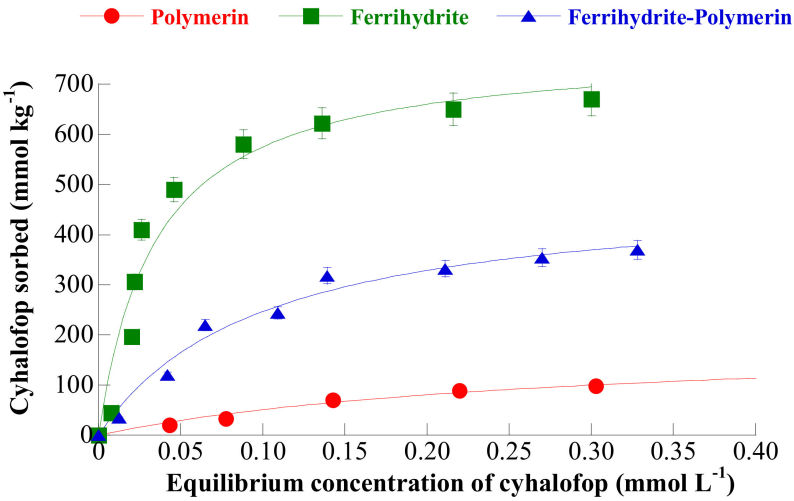

Figure 3. Adsorption isotherms of cyhalofop on polymeryn, ferrihydrite, and ferrihydrite-polymerin at the pH of maximum adsorption. Reproduced with permission from Sannino et al., *Journal of Agricultural and Food Chemistry*, published by the ACS, American Chemical Society, 2009.

Table 1. Highest paraquat, 2,4-D, and cyhalofop amounts adsorbed on polymerin at the appropriate agrochemical concentration and solid/liquid ratio (s/l).

s/l Ratio	Paraquat Concentration (mmol/L)	Adsorbed Paraquat (mmol/kg)
1/400	2.6	395
1/800	3.0	450
1/2000	2.5	800
s/l ratio	**2,4-D Concentration (mmol/L)**	**Adsorbed 2,4-D (mmol/kg)**
1/400	0.38	36
1/800	0.40	60
1/2000	0.40	140
s/l ratio	**CyhalofopConcentration (mmol/L)**	**Adsorbed Cyhalofop (mmol/kg)**
1/2000	0.32	90

Such amounts appear moderate. However, agrochemical adsorbed amounts at low agrochemical concentration do appear quite small. This datum appears very important from an applicative point of view, as agrochemical concentration levels in natural waters are usually decidedly low (lower than about 10 μmol/L) [15,16]. Moreover, this datum appears confirmed by the experiments of iterative agrochemical removal from water, at the pH of maximum adsorption, reported in Figures 4 and 5. Actually, a not reported residual agrochemical concentration (lower for paraquat, decidedly higher for 2,4-D and cyhalofop) remains in the water in spite of the fact that the agrochemical removal procedure was iterated from 3 to 8 times, at all the various s/l ratios [49,50]. The problem of the regeneration of the exhausted adsorbent is not considered as it can be composted with the destruction of the adsorbed agrochemicals.

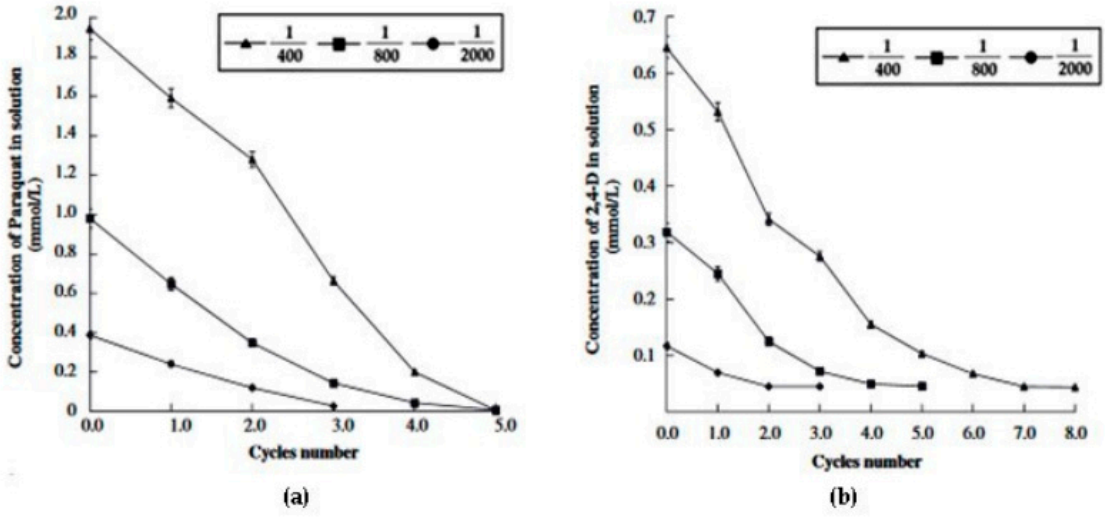

Figure 4. Residual paraquat (**a**) and 2,4-D (**b**) concentration as a function of the number of iterations, using polymeryn as adsorbent, at solid/liquid ratios of 1/2000, 1/800, and 1/400 at the pH of maximum adsorption. Reproduced with permission from Sannino et al., *Water Research*, published by Elsevier, 2008.

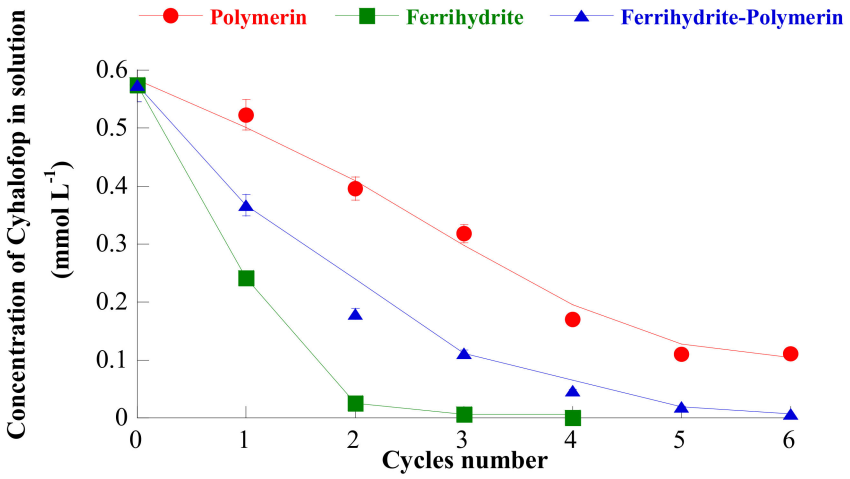

Figure 5. Residual cyhalofop concentration as a function of the number of iterations, using polymerin, ferrihydrite, and ferrihydrite-polymerin as adsorbents, at s/l = 1/2000 and at the pH of maximum adsorption. Reproduced with permission from Sannino et al., *Journal of Agricultural and Food Chemistry*, published by the ACS, 2009.

3.2. *Adsorption on Zeolite H-Y*

Removal of the agrochemical simazine from water by adsorption on zeolite H-Y was reported in [52,55,66].

The H-Y zeolite was chosen on the basis of these considerations: (1) the dimensions of the windows are similar to those of simazine [17,67], which allows its fast uptake [7]; (2) the presence of acid sites which can react with the lone electron pairs of simazine [68]; (3) the thermal stability [68]; (4) original Y zeolite is low cost and commercially available, as well as other zeolites such as zeolite A [69]. H-Y zeolite was prepared according to the procedure described in detail in [67,68]. The obtained H-Y zeolite was used to remove simazine by adsorption from distilled water and from a well water having the composition reported in Table 2.

Table 2. Features of the well water.

Parameter	Value
pH:	8.54
Conductivity (dS/m)	1.47
CO_3^{2-} (mg/L)	24.00
HCO_3^- (mg/L)	838.14
Cl^- (mg/L)	96.36
SO_4^{2-} (mg/L)	15.40
NO_3^- (mg/L)	36.51
NO_2^- (mg/L)	0.026
Na^+ (mg/L)	234.6
Ca^{2+} (mg/L)	54.86
K^+ (mg/L)	45.32
Mg^{2+} (mg/L)	31.85

Reproduced with permission from Sannino et al., *Journal of Environmental Science and Health*, PART B, Pesticides, Food Contaminants, and Agriculture Wastes, published by Taylor and Francis, 2015.

Interestingly, adsorption of simazine on H-Y zeolite resulted poorly affected by type of water used in the experiments, in that the pH at which the maximum simazine adsorption occurred was the same (5.5) in both types of water, as well as the amount of adsorbed simazine. Moreover, also adsorption isotherms of simazine from the two different waters were very similar (simazine adsorption isotherm from distilled water is reported in Figure 6) and kinetics of adsorption from both waters was pseudo-second order with the attainment of equilibrium in about one day [52,55,66]. These observations suggest that the mechanism of adsorption is independent of the type of water.

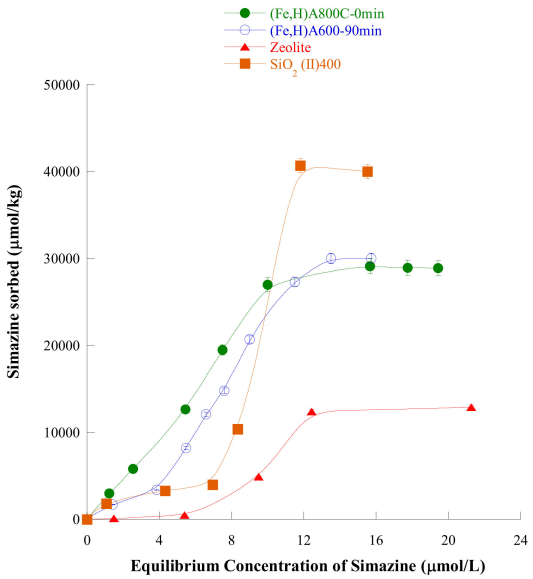

Figure 6. Adsorption isotherm of simazine on (Fe,H)A800C-0 min (full circles), (Fe,H)A600C-90 min (empty circles), zeolite HY (full triangle), and SiO2(II)400 (full square) samples at the pH of maximum adsorption. Reproduced with permission from Pansini et al., *Journal of Environmental Chemical Engineering*, published by Elsevier, 2018.

In particular, zeolite H-Y in water has only Brønsted acidic centers [68], as possible Lewis acidic centers have reacted. In turn, simazine behaves as a base because of the lone pairs on N atoms on the lateral chains. Thus, simazine uptake by zeolite H-Y can be considered as involving a typical acid-base equilibrium. Such interactions occur most favorably at a pH where the following two phenomena balance each other as:

1. at alkaline pH, hydroxyl anions neutralize the acid sites of H-Y zeolite, being the OH^- ion a stronger base than simazine (Figure 7a);
2. at acidic pH, the hydronium ions form reacts with the N lone pairs of simazine (Figure 7b).

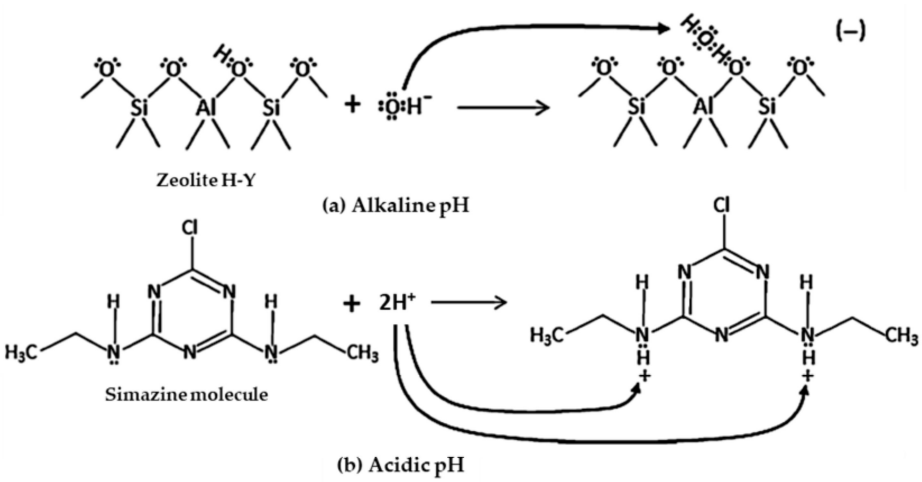

Figure 7. Mechanistic diagram to illustrate the adsorption mechanism of simazine on zeolite H-Y: H-Y zeolite framework (**a**) and simazine molecule (**b**) at alkaline and acidic pH, respectively. Reproduced with permission from Sannino et al., *Journal of Hazardous Materials*, published by Elsevier, 2012.

Adsorption isotherms of simazine from both distilled and well water (at the pH of maximum adsorption) showed a sigmoidal shape and were classified, according to [65] as of S-type and sloped to L-type. Its first concave portion may be analyzed according to the Freundlich equation. Moreover, a plateau of adsorbed simazine at about 12500 μmol/kg was recorded at equilibrium concentration not lower than about 12 μmol/L simazine. Despite this, being sigmoidal the shape of the isotherm, simazine adsorption at low simazine equilibrium concentration is modest. Despite this, the two-step (the first at s/l = 1/10000, the second at s/l = 1/10, at the pH of maximum adsorption) iterative procedure of simazine removal from (both distilled and well) water was able to bring residual simazine concentration in solution from 11 μmol/L (concentration at which agrochemicals are usually found in natural waters [15,16]) to below 0.05 mg/L ≈ 0.25 μmol/L (see Figure 8).

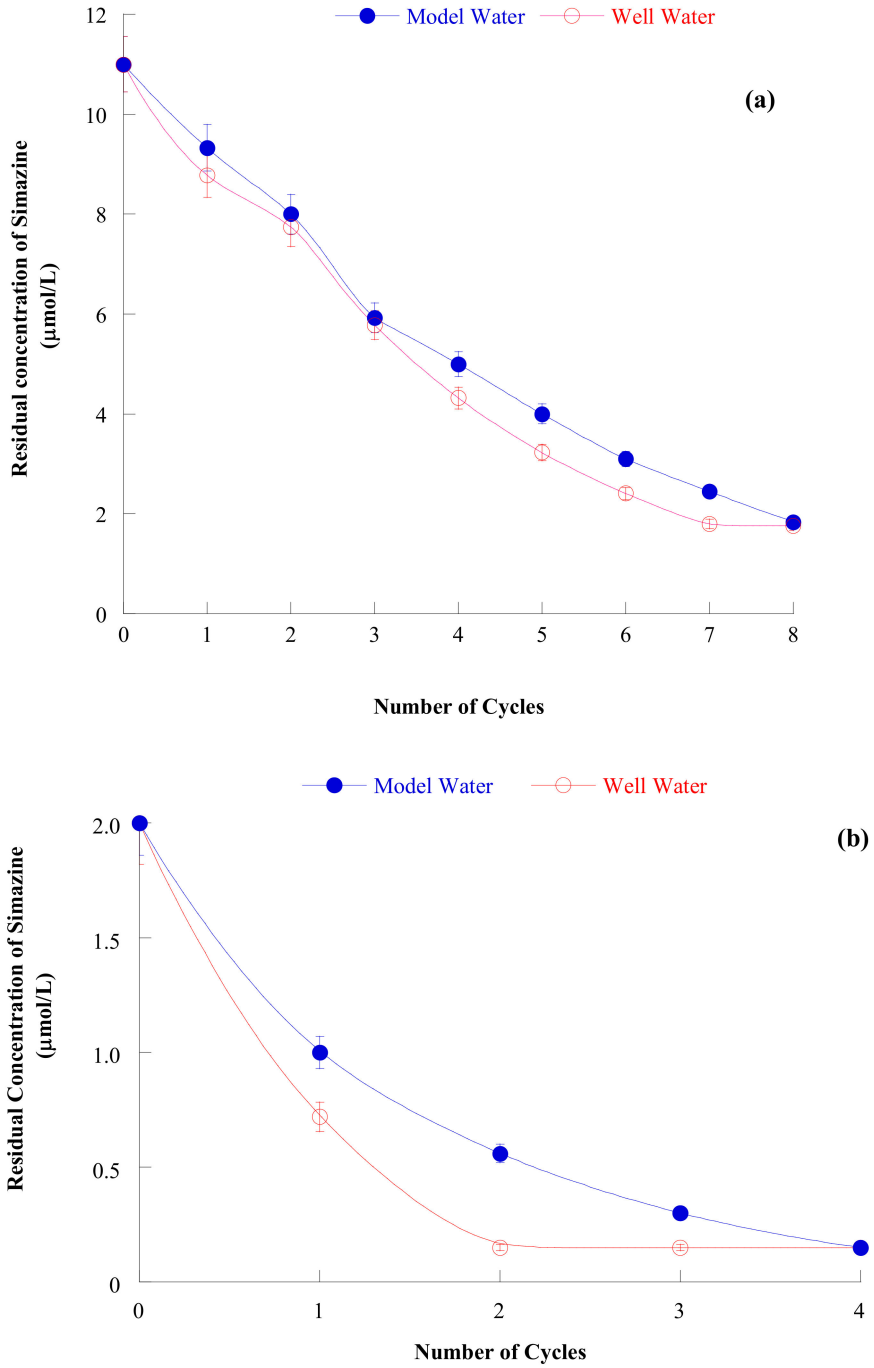

Figure 8. (**a**) Residual simazine concentration in the model water (full symbols) and well water (open symbols) as a function of the number of iteration of the iterative process, using zeolite H-Y (initial simazine concentration = 11 µmol/L, s/l ratio = 1/10000, pH = 6.5, contact time = 24 h). (**b**) Residual simazine concentration in the model water (full symbols) and well water (open symbols) as a function of the number of iteration of the iterative process, using zeolite H-Y (initial simazine concentration = 2 µmol/L, s/l ratio = 1/10, pH = 6.5, contact time = 24 h). Reproduced with permission from Sannino et al., *Journal of Environmental Science and Health*, PART B, Pesticides, Food Contaminants, and Agriculture Wastes, published by Taylor and Francis, 2015.

The attainment of this concentration appears of large practical importance as in Italy the DLGS. N. 152/2006 states 0.05 mg/L as the maximum concentration of agrochemicals allowed in wastewater to be released in surface waters or in sink.

The thermal regeneration of simazine-bearing exhausted zeolite H-Y was proposed. Actually, simazine was subjected to thermogravimetric (TG) and differential thermal analysis (DTA) in air and these curves were reported in [52]. It was found that:

1. The DTA curve exhibited a sharp endothermic peak at 239 °C and four small exothermic peaks in the temperature range 258–860 °C, and a final sharp exothermic peak at 500 °C.
2. A total weight loss larger than 95% was recorded through the TG analysis: it started at about 200 °C and attained completion at about 500 °C.

These findings were interpreted by considering that simazine undergoes thermal decomposition between 200 °C and 500 °C and that the moieties arising from its decomposition burn in the same temperature range. Thus, a few minutes thermal treatment at 500 °C of exhausted, simazine-bearing zeolite H-Y would result in the destruction of the agrochemical with no damage for the adsorbent which, during its preparation, was twice thermally treated at 550 °C for 3 h.

3.3. Adsorption on Porous Oxides

Adsorption of agrochemicals on various porous oxides was the subject of a series of interesting studies [21,48,50,51,53–57].

A composite adsorbent was produced by adding 0.1 M NaOH to an $AlCl_3$ and Na-saturated montmorillonite suspension, which gave rise to the precipitation of $Al(OH)_3$ over the montmorillonite surface [70]. After washing with distilled water and freeze-drying, a composite adsorbent, formed by a Na-saturated clay supporting an amphoteric oxo-hydroxide was obtained and used for the adsorption of 2,4-D from distilled water, at s/l = 1/20 and contact time = 24 h. Moreover, no indication of the pH of adsorption experiments was reported and thus, it appears likely that these experiments were performed at the pH naturally occurring when 2,4-D bearing solution and composite adsorbent were contacted.

It was found that, at saturation, about 900 μg of 2,4-D were adsorbed per gram of adsorbent; only 44% of adsorbed 2,4-D was removed from the adsorbent by means of two washing cycles of 24 h (0.1 M acetate, pH = 5.6) and, thus, the remaining 507 μg/g were stably chemisorbed. Apparently, the following two different mechanisms explained the physical and chemical sorption of 2,4-D: (1) electrostatic interactions between the COO^- moieties of 2,4-D and the positive sites of clays, and (2) ligand exchanges of COO^- groups with −OH or water at the clay surface, respectively.

In [50] another adsorbent was prepared as follows: a 0.1 M $FeCl_3$ solution was titrated to pH = 6 by adding 1 M NaOH. The precipitate was aged at 20 °C for 24 h and, subsequently centrifuged, washed, dialyzed against distilled water, and freeze dried, thus obtaining an iron oxo-hydroxide [$Fe(OH)_x$] known as ferrihydrite [71]. Then, 10 mg of this adsorbent were added to 20 mL of various solutions bearing cyhalofop (s/l = 1/2000). As far as the adsorption dependence on pH is concerned, the maximum amount cyhalofop adsorbed on ferrihydrite occurred at pH 3.5. At this pH, the surface of ferrihydrite is completely covered by positive charges (pH of zero charge = 9.4) and the un-ionized/ionized agrochemical is about 50/50%. In such conditions, carboxylate groups of cyhalofop formed H bonds with the positive surface of ferrihydrite. Thus, adsorption of cyhalofop on ferrihydrite attains its maximum at pH = 3.5, as: (1) at pH > 3.5 the surface of ferrihydrite is protonated to a lower extent; and (2) at pH < 3.5 the amount of un-ionized cyhalofop predominates on its ionized form. These hypotheses were confirmed by the DRIFTS spectra reported in [50].

Kinetic studies, at the pH of maximum adsorption, showed that adsorption of cyhalofop on ferrihydrite attained equilibrium in about 2 h and that the process was pseudo first order. The adsorption isotherm of cyhalofop on ferrihydrite (at the pH of maximum adsorption) (see Figure 3) was well fitted by the Langmuir equation and was found to lie far above the adsorption isotherms of cyhalofop on polymerin and on a complex polymerin-ferrihydrite [50], thus attaining a larger adsorbed amount (650 mmol/kg). Such a better cyhalofop adsorption ability of ferrihydrite was confirmed by experiments of iterative agrochemical removal from water at the pH of maximum adsorption: The data in Figure 5 show that the not-reported residual agrochemical concentration in water is decidedly

lower in the case of adsorption on ferrihydrite than in the case of adsorption on polymerin and on the polymerin-ferrihydrite complex and that such value is attained after a lower number of iterations [50]. Despite this, the fact that this value is not reported suggests that it is higher than the limits allowed by law (0.05 mg/L). The problem of the regeneration of the exhausted adsorbent is not investigated.

Unlike the porous oxides tested in refs. [48,50] which were produced in the laboratory, commercial samples of γ-alumina (γ—Al_2O_3) and iron(III) oxide (Fe_2O_3) (IoliTec Nanomaterials, 99.9% and 99.5% purity, respectively) were used for MCPA [21] and simazine [51] adsorption from water by adding 2.0, 10, 20, and 40 mg of oxides to a final volume of 20 mL of simazine bearing solution (s/l = 1/10,000, 1/2000, 1/1000 and 1/500, respectively). The textural properties of the commercial adsorbents were evaluated according to [72]. The most meaningful data are summarized in Table 3.

Table 3. Physical and chemical properties of Al_2O_3 and Fe_2O_3. BET: Brunauer–Emmett–Teller; SSA: Specific Surface Area; PZC: point of zero charge.

	Total Pore Volume (cm/g)	Particle Size (nm)	Average Pore Diameter (nm)	BET SSA (m/g)	PZC
γ-Al_2O_3	0.723	20	14.8	195	9.1
Fe_2O_3	0.239	10–00	9.2	106	10.1

Agrochemical adsorption dependence on pH was firstly investigated. MCPA optimum adsorption pH was 4.0 and 3.5, for Al_2O_3 and Fe_2O_3, respectively, whereas simazine optimum adsorption pH was 6.5 and 3.5 for Al_2O_3 and Fe_2O_3, respectively.

MCPA adsorption dependence on pH was explained by considering that, at the optimum adsorption pH of MCPA, the surface of both oxides is positively charged (Table 3) and the proportions of $COOH/COO^-$ groups were estimated as about 40%/60% and 50%/50%, for Al_2O_3 and Fe_2O_3, respectively. In these conditions, the ionized carboxylic groups of MCPA formed hydrogen bonds with the positive surface of both oxides.

Thus, adsorption of MCPA on Al_2O_3 and Fe_2O_3 attains its maximum at the reported values of pH (4.0 and 3.5 for Al_2O_3 and Fe_2O_3, respectively) as: (1) at higher pH the surface of both oxides is protonated to a lower extent; and (2) at lower pH the amount of un-ionized MCPA predominates in its ionized form.

Simazine adsorption dependence on pH appears different, as simazine in aqueous solution behaves as a weak base. Thus, adsorption on the two oxides appears related to the creation of hydrogen bond between thee N atoms of alkali side chains and the surface of the oxide. The different character of the oxides (decidedly amphoteric Al_2O_3 and more basic Fe_2O_3) gives rise to a higher pH of maximum adsorption for Al_2O_3 (6.5) than Fe_2O_3 (3.5). In this case at pH higher than the one of maximum adsorption the surface of both oxides is protonated to a lower extent and at pH lower than the one of maximum adsorption simazine is protonated to a larger extent which hinders its interaction with the positively charged surface of the adsorbent.

The uptakes of MCPA and simazine by γ—Al_2O_3 and Fe_2O_3 were recorded at various times and at the pH of maximum adsorption, in order to investigate the kinetics of the adsorption process. It was found that MCPA adsorption was fast on Al_2O_3 and slower on Fe_2O_3 (5 and 90 min to attain equilibrium, respectively), whereas the contrary occurred for simazine adsorption (120 and 5 min to attain equilibrium, respectively). Moreover, adsorption of MCPA on both oxides was found to follow pseudo first-order kinetics, whereas adsorption of simazine on the same oxides was found to follow pseudo second-order kinetics. The interpretation of these findings do not appear immediate, although it is apparent that the different acid/base properties of the two agrochemicals (MCPA is an acid and simazine is a base) seems to play a key role in determining different kinetic behavior. Figures 9 and 10 report the adsorption isotherm of MCPA and simazine (at the pH of maximum adsorption) on Al_2O_3 and Fe_2O_3, respectively.

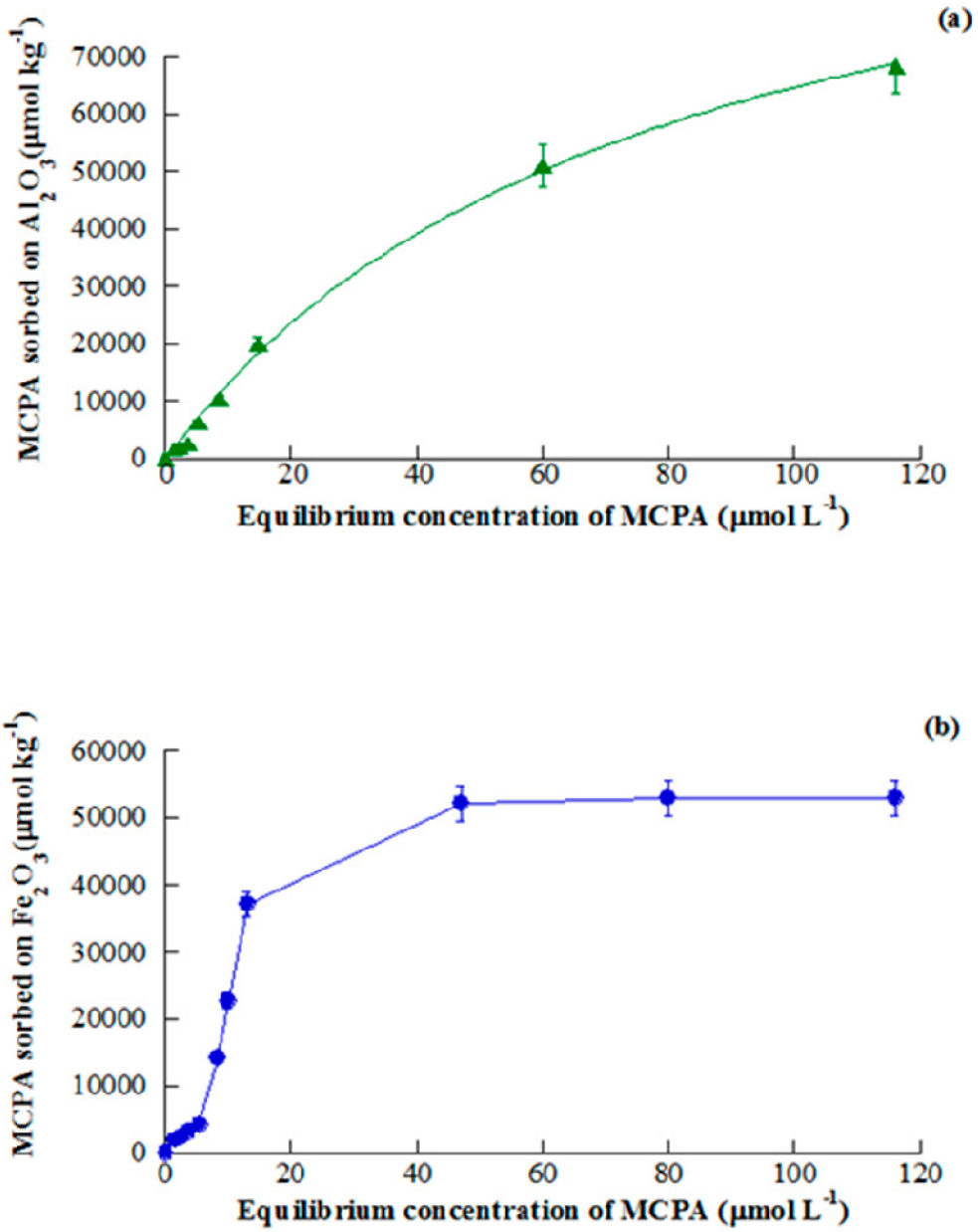

Figure 9. Adsorption isotherm of MCPA on Al_2O_3 (**a**) and Fe_2O_3 (**b**) at the pH of maximum adsorption. Reproduced with permission from Addorisio et al., *Journal of Agricultural and Food Chemistry*, published by the ACS, 2010.

The adsorption isotherms of the two agrochemicals on both oxides were curve-fitted by applying the Freundlich adsorption model. The classification of the isotherms according [65] is as follows: adsorption of MCPA on Al_2O_3 (L-type) and Fe_2O_3 (S-type); and adsorption of simazine on Al_2O_3 (S-type) and Fe_2O_3 (C-type). Only the isotherm of MCPA adsorption on Fe_2O_3 was performed so as to attain a plateau (50,000 µmol/kg at MCPA equilibrium concentration higher than 40 µmol/L). However, as previously said, the most important points of adsorption isotherm of agrochemicals, from the applicative point of view, are those at low equilibrium concentration as agrochemicals in natural waters and water bodies are present at concentrations lower than 10 µmol/L [15,16]. At such concentration levels the amount of agrochemical adsorbed on the porous oxide, used as adsorbents, ranges between 4000 and 12,000 µmol/kg and can be considered between modest and moderate.

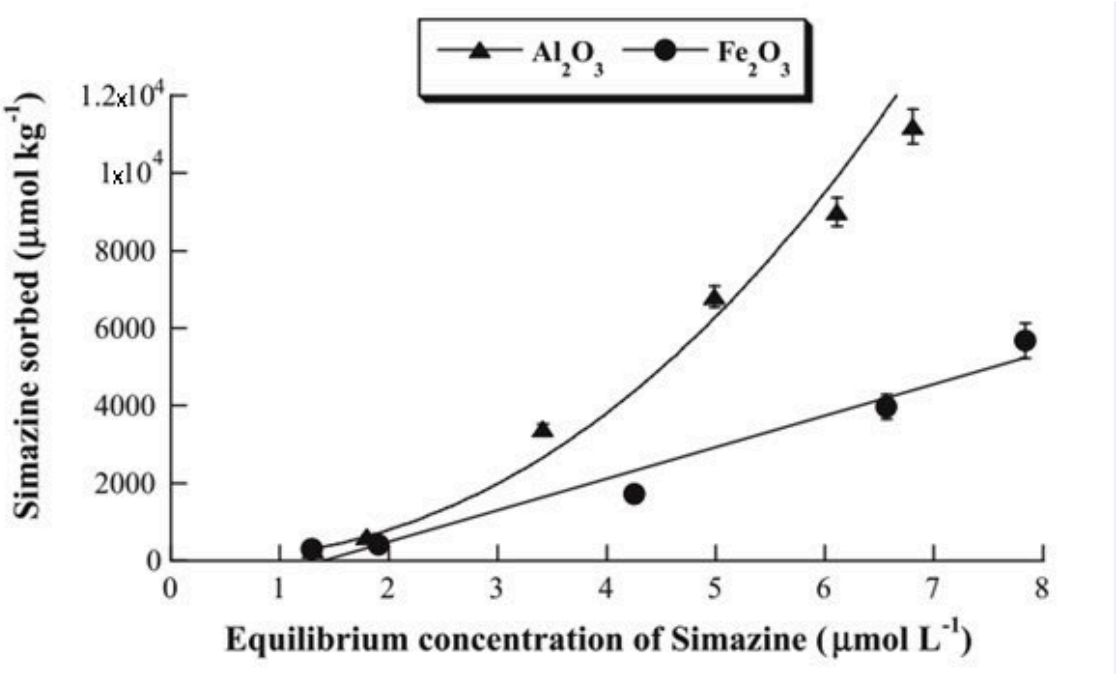

Figure 10. Adsorption isotherm of simazine on Al_2O_3 and Fe_2O_3 at the pH of maximum adsorption. Reproduced with permission from Addorisio et al., *Journal of Hazardous Materials*, published by Elsevier, 2011.

Finally, the results of the experiments of iterative removal of MCPA from water (at the pH of maximum adsorption and s/l = 1/10,000) on Al_2O_3 and Fe_2O_3 were reported in Figure 11.

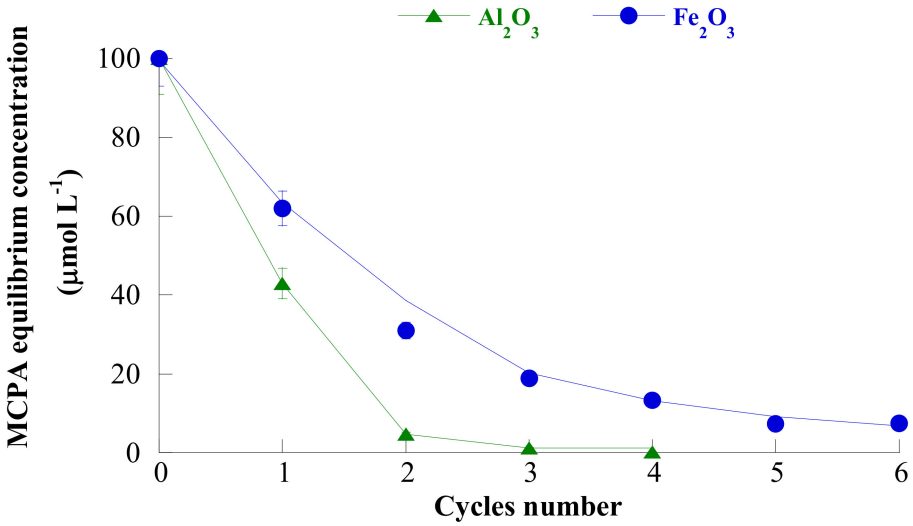

Figure 11. Residual MCPA concentration in the water as a function of the number of iteration of the iterative process, using Al_2O_3 (triangles) and Fe_2O_3 (circles) as adsorbents, at the pH of maximum adsorption. Reproduced with permission from Addorisio et al., *Journal of Agricultural and Food Chemistry*, published by the ACS, 2010.

It was found that MCPA concentration was brought from 100 µmol/L to a not reported residual value lower for adsorption on Al_2O_3 than on Fe_2O_3. Nevertheless, such residual value appears higher than the limits allowed by law.

The regeneration of the adsorbents after saturation with the agrochemicals was not addressed.

In the previous paragraphs, the adsorption of various agrochemicals on a basic oxide (Fe_2O_3) and an amphoteric oxide (Al_2O_3) was reviewed [21,48,50,51]. However, also the more acidic silicon dioxide

(SiO_2) was used to fulfil the same goal [53–57]. Actually, some samples of porous SiO_2 were prepared by the sol-gel technique according to [36,53]. The versatility of the sol-gel procedure allowed to tailor the porous network of SiO_2 to gain information about the relevance of micro/meso porosity on the adsorption processes of pesticides. To this purpose, a conventional sol-gel route and an alcohol-free method were designed considering different water to alkoxide ratios [36,41,53]. The procedures followed in preparing the samples of porous silica are described in detail in [53].

The porous SiO_2 sample that gave the best results in the adsorption of simazine from both distilled and natural water was the one labelled as SiO_2(II)400 for the sake of uniformity with [53].

The textural properties of the sample SiO_2(II)400 were evaluated according to [72]. The most meaningful data are the following: specific surface area 705 m^2/g, total pore volume 0.364 cm^3/g and micropore volume 0.056 cm^3/g [53].

Unlike zeolite H-Y, which showed very similar behavior in the adsorption of simazine both from distilled and well water, the adsorption capacity of simazine by sample SiO_2(II)400 was markedly affected by the presence of the interfering ions present in the well water (see Table 2). Actually, the pH of maximum simazine adsorption from distilled and well water was 5.5 and 4.5, respectively, and the amount of adsorbed simazine was about 29,000 and 15,000 μmol/kg, respectively [53,55]. Also, the isotherms of adsorption of simazine from distilled and well water (at the pH of maximum adsorption) were different: the former isotherm was reported in Figure 4, the latter (not reported) showed a similar trend of the former up to about 9 μmol/L equilibrium concentration, but, at slightly higher equilibrium concentration, rapidly attained a plateau at about 20,000 μmol/kg [53,55].

This plateau is about the half of the saturation value of the isotherm obtained in distilled water, reported in Figure 4. As far as kinetics of the process is concerned, nothing can be said as experiments of simazine adsorption at various times were performed only in distilled water at its pH of maximum adsorption (equilibrium was attained in about one hour and a pseudo second-order kinetic was followed) [53]. The interpretation of these finding appears very complicated as it involves a problem of simultaneous equilibrium in solution of overwhelming complexity. Thus, without claiming to give a valid explanation for whatever, it can be reasonably said that:

(1) Simazine uptake by porous SiO_2(II)400 is related to proton transfer from silanols (SiO-H) to simazine molecules, followed by electrostatic interactions holding together the negatively charged oxygen atoms of silanols and the positively charged protonated simazine molecules [53,55].
(2) Simazine uptake by porous SiO_2(II)400 attains its maximum at a pH value at which two phenomena balance each other. Actually, on the one hand, at alkaline pH, hydroxyl anions preferentially react with the hydrogen atoms of silanols, being OH^- a base stronger than simazine. On the other, at acidic pH, hydronium ions form substituted ammonium species by reacting with the lone pair electrons of nitrogen atoms of lateral chains of simazine molecule [53,55].

The above interpretation of simazine adsorption by porous SiO_2(II)400 suggests that CO_3^{2-} anions present in the well water could interfere with simazine adsorption. Actually, carbonate is a stronger base than simazine, and so could react with the silanol groups of SiO_2(II)400. These considerations account for the fact that the pH of maximum simazine adsorption shifts to more acidic pH value (from 5.5 to 4.5) when simazine adsorption on SiO_2(II)400 porous silica is performed from distilled or well water, respectively. Nevertheless, at this more acidic pH (4.5) simazine is protonated to a too large extent and, thus, the saturation of SiO_2(II)400 porous silica occurs at a simazine loading which is about the half of that recorded in distilled water [53,55].

Despite the fact that the whole adsorption process of simazine on silica seems affected by the kind of water (distilled or well) in which is performed, the two steps (the first at s/l = 1/10,000, the second at s/l = 1/100, at the pH of maximum adsorption) iterative procedure of simazine removal from (both distilled and well) water do not seem largely affected by this fact (see Figure 12).

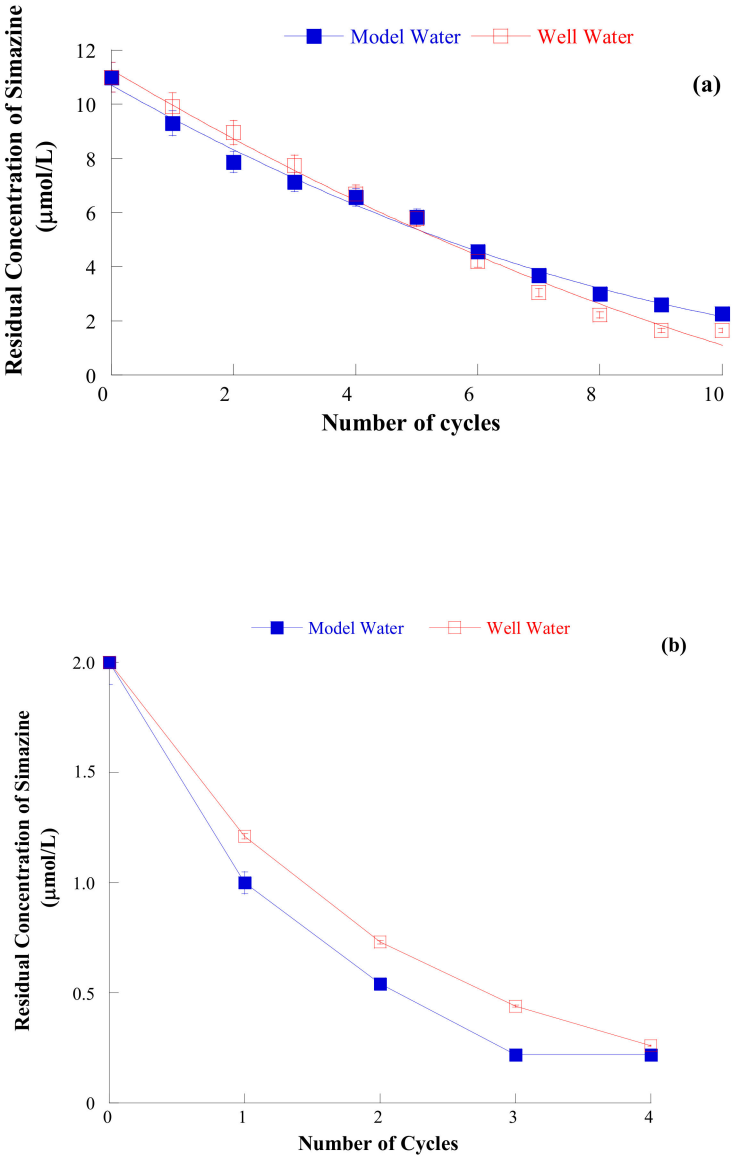

Figure 12. (**a**) Residual simazine concentration in the model water (pH = 5.5, full symbols) and well water (pH = 4.5, open symbols) as a function of the number of iteration of the cyclic process, using SiO2(II)400 porous silica (initial simazine concentration = 11 µmol/L, s/l ratio = 1/10,000, contact time = 24 h). (**b**) Residual simazine concentration in the model water (pH = 5.5, full symbols) and well water (pH = 4.5, open symbols) as a function of the number of iteration of the cyclic process, using SiO2(II)400 porous silica (initial simazine concentration = 2.0 µmol/L, s/l ratio = 1/100, contact time = 24 h). Reproduced with permission from Sannino et al., *Journal of Environmental Science and Health*, PART B, Pesticides, Food Contaminants, and Agriculture Wastes, published by Taylor and Francis, 2015.

This finding may be explained by considering that at the (low) simazine concentration used during these runs the interfering action of ions in water does not play a crucial role.

Examining data of Figure 10, it may be found that the iterative procedure was able to bring the residual simazine concentration in solution from 11 µmol/L (concentration at which agrochemicals are usually found in natural waters [15,16]) to below 0.05 mg/L ≈ 0.25 µmol/L.

The attainment of this residual concentration appears of large practical importance as in Italy the DLGS. N. 152/2006 states 0.05 mg/L as the maximum concentration of agrochemicals allowed in wastewater to be released in surface waters or in sink [53,55].

A thermal regeneration (few minutes at about 500 °C) of the exhausted, simazine bearing, adsorbent similar to the one described for zeolite H-Y may be proposed as thermal treatment up to 600 °C were not found to affect the adsorptive properties of SiO_2(II)400 porous silica sample [53,55].

3.4. Adsorption on Magnetic Metal-Ceramic Nanocomposites

Some year ago a smart process to obtain magnetic nanocomposites from commercial zeolites was protected by the application of a patent [73,74]. The first step of this process consists of an ionic exchange of the zeolite with a heavy metal (Ni, Fe or Co), whereas the second step is a thermal treatment at relatively mild temperature (500–050 °C) under reducing atmosphere, obtained by flowing a 2.0 vol. % H_2 in Ar mixture. The materials resulting from this process are formed by a dispersion of magnetic metal (Ni, Fe, or Co) nanoparticles (size ranging between 5 and 25 nm) embedded in a ceramic matrix mainly based on amorphous silica and alumina [75–77]. Obtained nanocomposites, which exhibit magnetic properties owing to the presence of Ni, Fe, or Co nanoparticles [78–80], showed also good adsorptive ability, and thus were advantageously used in the DNA separation [81] and agrochemical removal from water by adsorption [58]. Actually, in this last [58] two different magnetic adsorbents, produced with the reported process, were used to remove simazine from distilled water by adsorption. Figure 13 shows the sequence of operations performed in the preparation of the two magnetic nanocomposites used in simazine removal from water by adsorption. The description of the details of this sequence of operations can be found in [58,82].

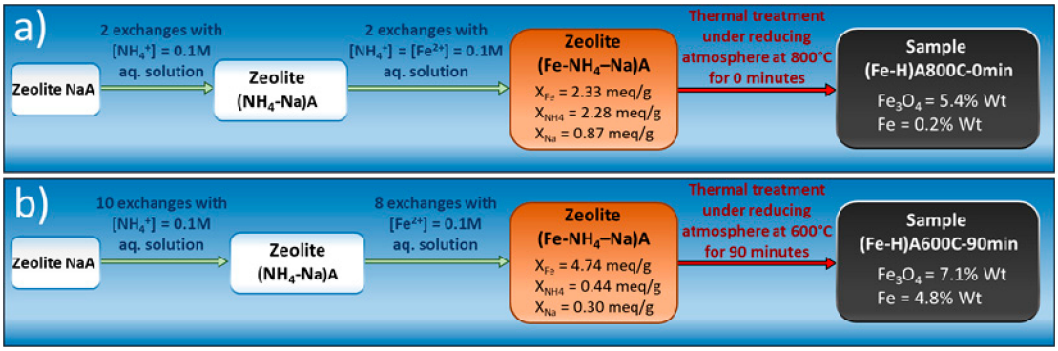

Figure 13. Preparation of magnetic adsorbents (**a**) (Fe,H)A800C-0 min. and (**b**) (Fe,H)A600C-90 min. Reproduced with permission from Pansini et al., *Journal of Environmental Chemical Engineering*, published by Elsevier, 2018.

These two samples of nanocomposites were subjected to quantitative phase determinations by the combined RIR-Rieveld method [83–85] which gave the results summarized in Table 4.

Table 4. Quantitative Phase analysis of samples (Fe,H)A800C-0 min. and (b) (Fe,H)A600C-90 min (values are reported in wt.%).

Sample	LTA_Fe%	Magnetite%	Wustite%	Fe%	Amorphous Phase%
(Fe,H)A600C-90 min	0.8(3)	7.1(3)	0.2(1)	4.8(1)	87.1
(Fe,H)A800C-0 min	8.0(2)	5.4(1)	/	0.2(1)	86.4

Reproduced with permission from Pansini et al., *Journal of Environmental Chemical Engineering*, published by Elsevier, 2018.

Moreover, these two samples of nanocomposites were subjected to: (1) textural and morphological characterization, whose main results are summarized in Table 5; (2) TEM characterization.

Table 5. Specific surface area (S_{BET}), total pore volume (V_p), and micropore volume (V_{mp}).

Sample	S_{BET} (m^2/g)	V_p (cm^3/g)	V_{mp} (cm^3/g)
(Fe,H)A600C-90 min	28	0.15	/
(Fe,H)A800C-0 min	19	0.13	/

Reproduced with permission from Pansini et al., *Journal of Environmental Chemical Engineering*, published by Elsevier, 2018.

In particular, Figure 14a,b shows some TEM images of samples (Fe,H)A800C-0 min and (Fe,H)A600C-90 min, where nanoparticles of magnetite and Fe^0 appear dark. The histograms of the nanoparticle size distribution reveal that their average dimension is 11 and 1.82 nm for samples (Fe,H)A800C-0 min and (Fe,H)A600C-90 min, respectively. A more detailed description of TEM images is reported in [58].

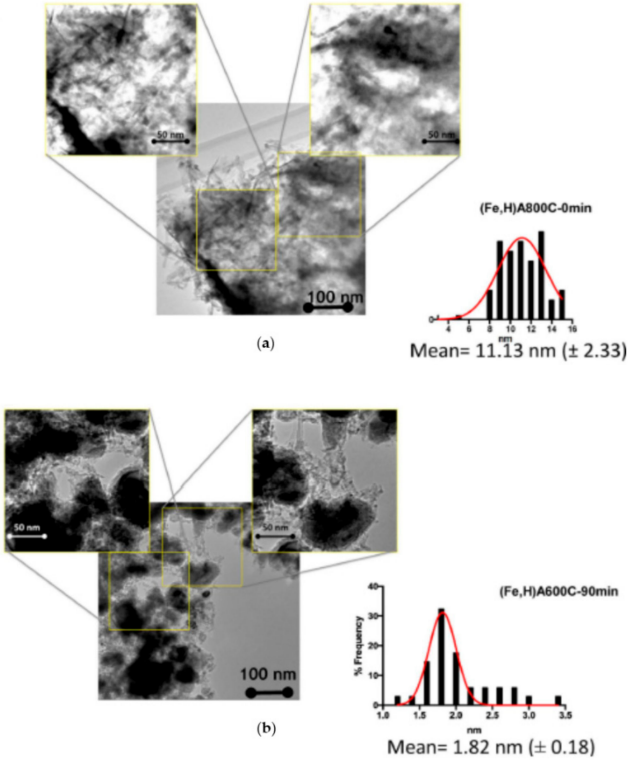

Figure 14. Representative TEM (Transmission Electron Microscopy) images of (**a**) sample FeA800C-0 min and (**b**) sample (Fe,H)A600C-90 min. Reproduced with permission from Pansini et al., *Journal of Environmental Chemical Engineering*, published by Elsevier, 2018.

The results of the magnetic characterization to which the two magnetic adsorbents studied in this work were subjected, were reported in Figure 15 where the magnetic hysteresis cycles of (Fe,H)A800C-0 min (red symbols) and (Fe,H)A600C-90 min (black symbols) are shown. Magnetization values (M) of 4.2 and 12.3 emu/g, respectively, were recorded at the maximum applied field; it must be noted that complete magnetic saturation is not attained at 17 kOe, as expected from nanoparticulate systems.

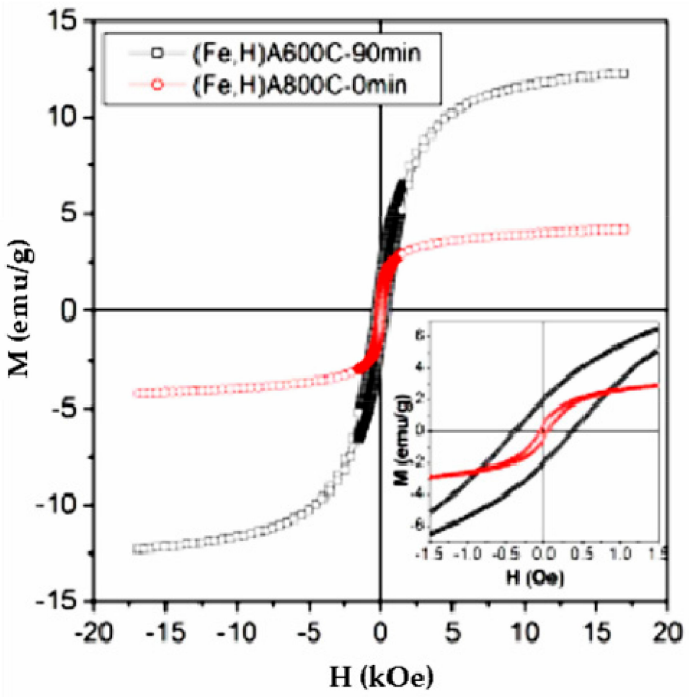

Figure 15. Room-temperature magnetic hysteresis loops of (Fe,H)A800C-0 min (red symbols) and (Fe,H)A600C-90 min (black symbols); inset: low-field region. Reproduced with permission from Pansini et al., *Journal of Environmental Chemical Engineering*, published by Elsevier, 2018.

Different coercive fields (H) are reported in the magnetization cycles. The magnetic adsorbent (Fe,H)A800C-0 min, which bears a considerable amount of magnetite, has a coercivity typical of Fe_3O_4 nanoparticles (≅45 Oe), whereas the coercive field of the magnetic adsorbent (Fe,H)A600C-90 min (H ≅ 375 Oe) is fully compatible with the presence of higher-anisotropy nanoparticles of metallic Fe (see Table 4). It is noteworthy that similar results concerning M, H, and the non-saturating character of magnetization curves of various Fe nanoparticles systems, obtained through different procedures, are reported in the literature [86,87]. The unsaturating M(H) curve indicates that a fraction of Fe ions remains dissolved in the host. Such magnetic features ensure an easy and fast magnetic separation of the exhausted adsorbent from the liquid phase, in which they were dispersed, by the use of a magnetic-field gradient produced by an external magnet.

As far as the dependence of simazine uptake by samples (Fe,H)A800C-0 min and (Fe,H)A600C-90 min on pH is concerned, it was found that about 25,000 μmol/kg were adsorbed on them at pH 6.5 and 3.0, respectively (s/l = 1/10,000). The fact that this maximum occurs at largely different pH values indicates that samples (Fe,H)A800C-0 min and (Fe,H)A600C-90 min adsorb simazine following largely different mechanisms. In particular, it was found that: (1) the adsorption of simazine on sample (Fe,H)A800C-0 min occurred according to the same mechanism of simazine adsorption on zeolite H-Y (see the final part of paragraph concerning adsorption on zeolite H-Y); (2) the adsorption of simazine on sample (Fe,H)A600C-90 min occurred through the formation of intermolecular hydrogen bond in the simazine-magnetite, or possibly even simazine-silica, contact layer as confirmed in [81,88,89]. The details of the mechanism of simazine adsorption are reported in [58].

Simazine isotherm of adsorption on samples (Fe,H)A800C-0 min and (Fe,H)A600C-90 min are reported in Figure 4, together with simazine adsorption isotherms on other adsorbents. In all these isotherms different adsorption plateaux are recorded: 12,000 μmol/L for zeolite H-Y, 30,000 μmol/L for samples (Fe,H)A800C-0 min and (Fe,H)A600C-90 min and 40,000 μmol/L for silica sample SiO_2(II)400. These values could suggest the consideration that magnetic samples (Fe,H)A800C-0 min and (Fe,H)A600C-90 min remove simazine from water more poorly than silica sample SiO_2(II)400. A more careful examination of these data shows that this conclusion is wrong. Actually, it must be

borne in mind that: (1) Agrochemicals are usually present in water bodies at concentrations lower than 10 μmol/L [15,16]; (2) the law limit is 0.05 mg/L ≈ 0.25 μmol/L. These considerations suggest that an adsorbent, viable for practical applications, whose task is removing simazine from water, must work well in the simazine concentration range from about 9–90 μmol/L to below 0.25 μmol/L. In this particular simazine concentration range, magnetic adsorbents (Fe,H)A800C-0 min and (Fe,H)A600C-90 min are found to exhibit the best performances. Actually, their adsorption isotherm lies far above than those of silica sample SiO_2(II)400 and zeolite H-Y. Moreover, the supplementary data concerning simazine adsorption on other adsorbents reported in [51,52] show that the magnetic adsorbents of this work exhibit an higher efficiency in simazine removal from water.

The kinetic runs and the results of the iterative process of simazine removal from water (Figures 16 and 17) further confirm the good efficiency of magnetic adsorbents (Fe,H)A800C-0 min and (Fe,H)A600C-90 min in the simazine removal from water.

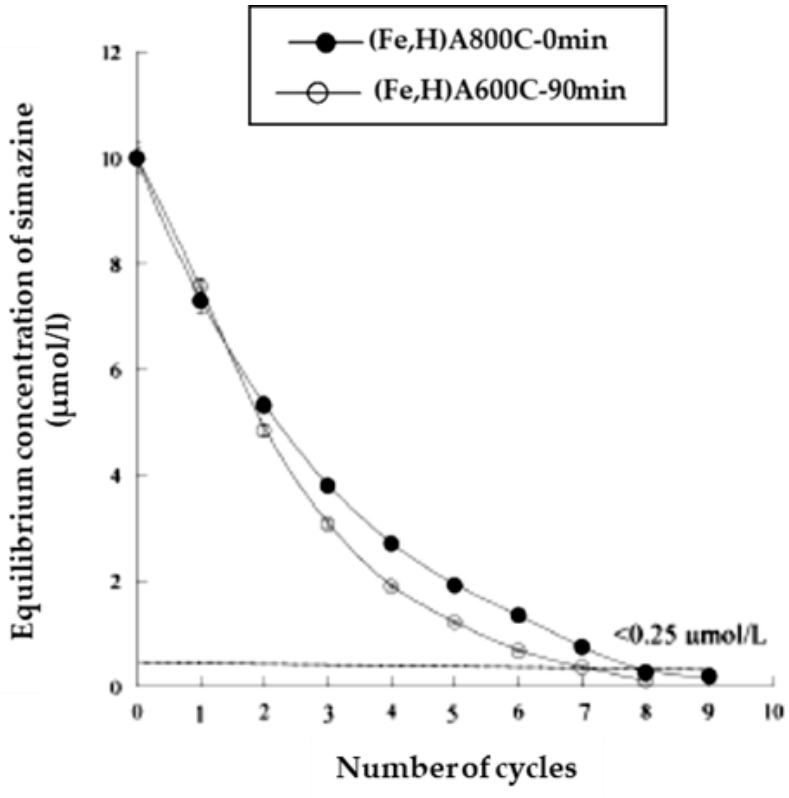

Figure 16. Iterative process of simazine removal from waters (s/l ratio = 1/10000, for 24 h, maximum adsorption pH). Reproduced with permission from Pansini et al., *Journal of Environmental Chemical Engineering*, published by Elsevier, 2018.

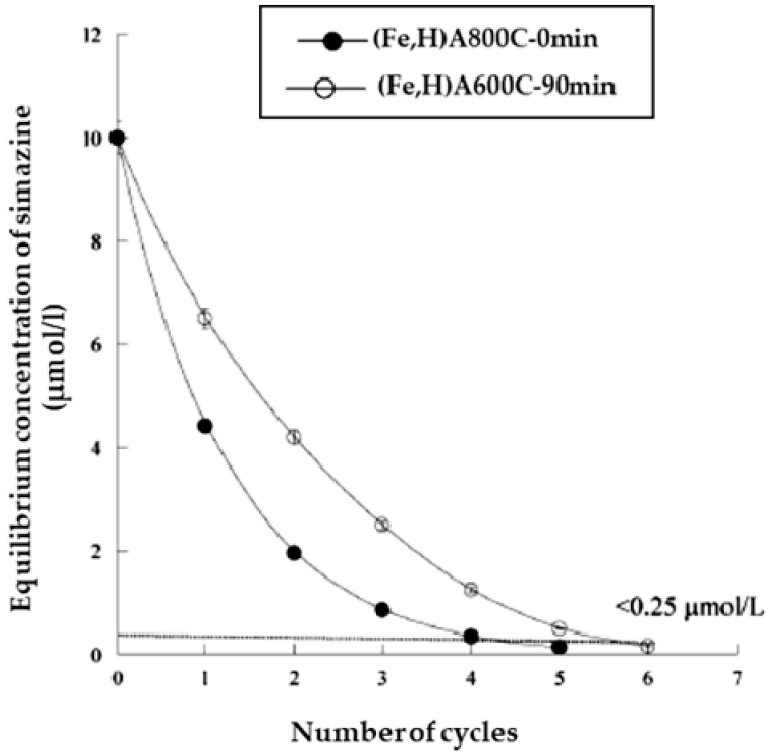

Figure 17. Iterative process of simazine removal from waters (s/l ratio = 1/1000, for 1.5 h, maximum adsorption pH). Reproduced with permission from Pansini et al., *Journal of Environmental Chemical Engineering*, published by Elsevier, 2018.

Regarding kinetic runs it was found that simazine adsorption on samples (Fe,H)A800C-0 min and (Fe,H)A600C-90 min followed a second order kinetics and that the time necessary to attain equilibrium was one day. However, it was also found that about 1.5–5 h were sufficient to attain a simazine uptake higher than about 70% for both samples. Regarding the iterative process, Figure 14 reports that 7–7 iterations (at s/l = 1/10,000 g/g and 24 h contact time) are sufficient to bring simazine concentration below the law limit (0.25 μmol/L), whereas Figure 15 shows that 5–5 iterations (at s/l = 1/1000 g/g and 1.5 h contact time) are sufficient to attain the same goal.

A thermal regeneration (few minutes at about 500 °C) of the exhausted, simazine bearing adsorbent similar (but not equal) to the one described for zeolite H-Y and SiO_2(II)400 porous silica sample may be proposed. Actually, such thermal treatment in air would result in the oxidation of the metallic iron with the possible loss of the magnetic properties of the adsorbents. This problem may be easily solved by performing this short thermal treatment under inert (created by N_2) or reducing (created by 2.0 vol. % H_2 in Ar mixture) atmosphere. In these conditions the magnetic adsorbents do not undergo any transformation as they were produced at a temperature decidedly higher than the one of the thermal treatment of regeneration (500 °C).

4. Conclusions

This review represents a sort of "ride" through the different views that the scientific community has towards the serious environmental problem created by presence of agrochemicals in natural waters and water bodies. What appears a little surprising is that, in a lag of time of about ten years, the attitude of the scientific community towards this problem has largely changed, thus showing a commendable enhanced sensitivity that pushed research in the direction of preparing more efficient and functional adsorbents. Actually, about ten years ago, acknowledged scientific journals published works concerning the removal of agrochemicals using humic-like substances waste of food industry. This view was originated by the "romantic" claim of solving the environmental problems with something

(the waste of the food industry) for which disposal was an environmental problem, thus "killing two birds with one stone". Obviously, this very attractive resolution has failed on account of the modest agrochemical removal ability and not sufficiently low agrochemical residual concentration in water that can be attained using humic-like substances as adsorbents. Thus, adsorbents exhibiting better and better performances in removing agrochemicals from water (such as properly modified zeolites and the porous oxides of various elements) were produced and tested, obtaining also very good results such as the attainment of agrochemicals concentration allowed by law. In particular, this last result must be kept in due consideration as, given the strong toxicity of agrochemicals, such limits are always very low (see the DLGS. N. 152/2006 ruling in Italy) and attainable with great difficulty. However, a method to solve an environmental problem is practical only if it can be simply and easily operated. Unfortunately, the separation of the exhausted adsorbent from the medium, after removal of agrochemicals, is a problem of overwhelming complexity at an industrial level. This point, in particular, seems to strongly suggest the use of magnetic adsorbents for the adsorption of agrochemicals from water. Actually, the simplicity of the magnetic separation from the aqueous medium by the use of an external magnet, the good performance in agrochemical removal, and the ease of regeneration concur, pointing to the magnetic adsorbents described in this work as being very promising candidates for the treatment of waters polluted by the presence of agrochemicals.

Nevertheless, it must be said that, despite the strength of all the above considerations, large-scale field applications of magnetic metal-ceramic nanocomposites in environmental decontamination are not reported in the literature, to the best of our knowledge, as confirmed by [90,91]. Furthermore, these two valuable works evidence that, among the various obstacles that the use of magnetic metal-ceramic nanocomposites in environmental decontamination encounters, the main issues are those regarding their commercialization, which appear, at the moment, to particularly hinder their use in practical application of a wider scale.

Author Contributions: Methodology, A.M., F.S., S.E., B.B., P.A., P.T. and G.B.; Validation, F.S.; Formal Analysis, G.D., F.S., B.B., P.T. and G.B.; Investigation, A.M., G.D., F.S., S.E., B.B. and P.A.; Resources, A.M., F.S. and S.E.; Writing-Original Draft Preparation, G.D. and M.P.; Writing-Review & Editing, F.S. and S.E.; Supervision, M.P. All authors have read and agreed to the published version of the manuscript.

Funding: This research received no external funding.

Conflicts of Interest: The authors declare no conflict of interest. The authors declared that they have obtained permissions for all the results that they used from a (foreign) periodical. The authors declare that all the figures and tables in this manuscript have obtained permission from the copyright owners for both the printed and online format.

References

1. Srivastava, B.; Jhelum, V.; Basu, D.D.; Patanjali, P.K. Adsorbents for pesticide uptake from contaminated water. *J. Sci. Ind. Res.* **2009**, *68*, 839–850.
2. Derylo-Marczewska, A.M.; Blachnio, A.; Marczewski, W.; Tarasiuk, B. Adsorption of selected herbicides from aqueous solutions on activated carbon. *J. Therm. Anal. Calorim.* **2010**, *101*, 785–794. [CrossRef]
3. Freyria, F.S.; Geobaldo, F.; Bonelli, B. Nanomaterials for the Abatement of Pharmaceuticals and Personal Care Products from Wastewater. *Appl. Sci.* **2018**, *8*, 170. [CrossRef]
4. Chigombe, P.; Saha, B.; Wakeman, R.J. Sorption of atrazine on conventional and surface modified activated carbons. *J. Colloid Interface Sci.* **2006**, *302*, 408–416. [CrossRef]
5. Mahalakashmi, M.; Vishnu Priya, S.; Arabindoo, B.; Palanichamy, M.; Murugesan, V. Photocatalytic degradation of aqueous propoxur solution using TiO_2 and Hβ zeolite-supported TiO_2. *J. Hazard. Mater.* **2009**, *161*, 336–343. [CrossRef]
6. Damjanovic, L.; Rakic, V.; Rac, V.; Stosic, D.; Aurox, A. The investigation of phenol removal from aqueous solutions by zeolite as solid adsorbents. *J. Hazard. Mater.* **2010**, *184*, 477–484. [CrossRef]
7. Ellis, J.; Korth, W. Removal of geosmin and methylisoborneol from drinking water by adsorption on ultrastable zeolite-Y. *Water Res.* **1993**, *4*, 535–539. [CrossRef]

8. Tsai, W.T.; Hsien, K.J.; Hsu, H. Adsorption of organic compounds from aqueous solution onto the synthesized zeolite. *J. Hazard. Mater.* **2009**, *161*, 635–641. [CrossRef]
9. Salvestrini, S.; Sagliano, P.; Iovino, P.; Capasso, S.; Colella, C. Atrazine adsorption by acid-activated zeolite-rich tuffs. *Appl. Clay Sci.* **2010**, *49*, 330–335. [CrossRef]
10. Cruz-Guzman, M.; Celis, R.; Carmen Hermosin, M.; Koskinen, W.C.; Cornejo, J. Adsorption of pesticides from water by functionalized organobentonites. *J. Agric. Food Chem.* **2005**, *53*, 7502–7511. [CrossRef]
11. Shankar, M.V.; Cheralathan, K.K.; Arabindoo, B.; Palanichamy, M.; Murugesan, V. Enhanced photocatalytic activity for the destruction of monocrotophos pesticide by TiO_2-Hβ. *J. Mol. Catal. A: Chem.* **2004**, *223*, 195–200. [CrossRef]
12. Shankar, M.V.; Anandan, S.; Venkatachalam, N.; Arabindoo, B.; Murugesan, V. Fine route for an efficient removal of 2,4-dichlorophenoxyacetic (2,4-D) by zeolite supported TiO_2. *Chemosphere* **2006**, *63*, 1014–1021. [CrossRef]
13. Lemic, J.; Kovacevic, D.; Tomasevic-Canovic, M.; Stanic, T.; Pfend, R. Removal of atrazine, lindane and diazinone from water by organo-zeolites. *Water Res.* **2006**, *40*, 1079–1085. [CrossRef]
14. Sprynskyy, M.; Ligor, T.; Buszewski, B. Clinoptilolite study of lindane and aldrin sorption processes from water solution. *J. Hazard. Mater.* **2008**, *151*, 570–577. [CrossRef]
15. Carlson, D.L.; Than, K.D.; Lynn Roberts, A. Acid- and base-catalyzed hydrolysis of chloroacetamide herbicides. *J. Agric. Food Chem.* **2006**, *54*, 4740–4750. [CrossRef]
16. Ignatowicz-Owsieniuk, K.; Skoczko, I. Dependance of sorption of phenoxyacetic herbicides on their physico-chemical properties. *Pol. J. Environ. Stud.* **2002**, *11*, 339–344.
17. Chen, S.S.; Taylor, J.S.; Mulford, L.A. Influences of molecular weight, molecular size, flux, and recovery for aromatic pesticides removal by nanofiltration membranes. *Desalination* **2004**, *160*, 103–111. [CrossRef]
18. Wang, S.; Peng, Y. Natural zeolites as effective adsorbents in water and wastewater treatment. *Chem. Eng. J.* **2010**, *156*, 11–24. [CrossRef]
19. Paul, B.; Yang, D.; Yang, X.; Ke, X.; Frost, R.; Zhu, H. Adsorption of the herbicide simazine on moderately acid-activated beidellite. *Appl. Clay Sci.* **2010**, *49*, 80–83. [CrossRef]
20. De Smedt, C.; Ferrer, F.; Leus, K.; Spanoghe, P. Removal of pesticides from aqueous solutions by adsorption on zeolite sas solid adsorbents. *Adsorpt. Sci. Technol.* **2015**, *33*, 457–485. [CrossRef]
21. Addorisio, V.; Esposito, E.; Sannino, F. Sorption capacity of mesoporous metal oxides for the removal of MCPA from polluted waters. *J. Agric. Food Chem.* **2010**, *58*, 5011–5016. [CrossRef] [PubMed]
22. Foo, K.Y.; Hameed, B.H. Review Detoxification of pesticide waste via activated carbon adsorption process. *J. Hazard. Mater.* **2010**, *175*, 1–11. [CrossRef] [PubMed]
23. Hesket, N.; Jones, N.M.; Tipping, E. The interaction of some pesticides and herbicides with humic substances. *Anal. Chim. Acta* **1996**, *327*, 191–201. [CrossRef]
24. Celi, L.; Gennari, M.; Khan, S.U.; Schnitzer, M. Mechanism of acifluorfen interaction with humic acid. *Soil Sci. Soc. Am. J.* **1997**, *61*, 1659–1665. [CrossRef]
25. Akhtar, M.; Hasany, S.M.; Bhanger, M.I.; Iqbal, S. Low cost sorbents for the removal of methyl parathion pesticide from aqueous solutions. *Chemosphere* **2007**, *66*, 1829–1838. [CrossRef]
26. Ćwieląg-Piasecka, I.; Medyńska-Juraszek, A.; Jerzykiewicz, M.; Dębicka, M.; Bekier, J.; Jamroz, E.; Kawałko, D. Humic acid and biochar as specific sorbents of pesticides. *J. Soil. Sediment.* **2018**, *18*, 2692–2702. [CrossRef]
27. Büyüksönmez, F.; Rynk, R.; Hess, T.F.; Bechinski, E. Occurrence, Degradation and Fate of Pesticides during Composting Part II: Occurrence and Fate of Pesticides in Compost and Composting Systems. *Compost Sci. Util.* **2000**, *8*, 61–81. [CrossRef]
28. Semple, K.T.; Reid, B.J.; Fermor, T.R. Impact of composting strategies on the treatment of soils contaminated with organic pollutants. *Environ. Pollut.* **2001**, *112*, 269–283. [CrossRef]
29. Karanasios, E.; Tsiropoulos, N.G.; Karpouzas, D.G.; EHALIOTIS, C. Degradation and Adsorption of Pesticides in Compost-Based Biomixtures as Potential Substrates for Biobeds in Southern Europe. *J. Agric. Food Chem.* **2010**, *58*, 9147–9156. [CrossRef]
30. Colella, C.; de' Gennaro, M.; Langella, A.; Pansini, M. Evaluation of Italian natural zeolites in wastewater treatment: Cu and Zn exchange reaction on phillipsite and chabazite. *Sep. Sci. Technol.* **1998**, *33*, 467–481. [CrossRef]
31. Pansini, M.; Colella, C. Dynamic data on lead uptake from water by chabazite. *Desalination* **1990**, *78*, 287–295. [CrossRef]

32. Esposito, S.; Marocco, A.; Dell'Agli, G.; de Gennaro, B.; Pansini, M. Relationships between the water content of zeolites and their cation population. *Microporous Mesoporous Mater.* **2015**, *202*, 36–43. [CrossRef]
33. Marocco, A.; Liguori, B.; Dell'Agli, G.; Pansini, M. Sintering behaviour of celsian based ceramics obtained from the thermal conversion of (Ba, Sr)-exchanged zeolite A. *J. Eur. Ceram. Soc.* **2011**, *31*, 1965–1973. [CrossRef]
34. Albino, V.; Cioffi, R.; Pansini, M.; Colella, C. Disposal of lead-containing zeolite sludges in cement matrix. *Environ. Technol.* **1995**, *16*, 147–165. [CrossRef]
35. Albino, V.; Cioffi, R.; Pansini, M.; Colella, C. Evaluation of cement-based solidified materials encapsulating Cd-exchanged natural zeolites. *Environ. Technol.* **1996**, *17*, 1215–1224.
36. Esposito, E. "Traditional" sol-gel chemistry as a powerful tool for the preparation of supported metal and metal oxide catalysts. *Materials* **2019**, *12*, 668. [CrossRef]
37. Bagnasco, G.; Cammarano, C.; Turco, M.; Esposito, S.; Aronne, A.; Pernice, P. TPR/TPO characterization of cobalt-silicon mixed oxide nanocomposites prepared by sol-gel. *Thermochim. Acta* **2008**, *471*, 51–54. [CrossRef]
38. Esposito, S.; Setaro, A.; Maddalena, P.; Aronne, A.; Pernice, P.; Laracca, M. Synthesis of cobalt doped silica thin film for low temperature optical gas sensor. *J. Sol-Gel Sci. Technol.* **2011**, *60*, 388–394. [CrossRef]
39. Esposito, S.; Turco, M.; Bagnasco, G.; Cammarano, C.; Pernice, P. New insight into the preparation of copper/zirconia catalysts by sol-gel method. *Appl. Catal. A Gen.* **2011**, *403*, 128–135. [CrossRef]
40. Minieri, L.; Esposito, S.; Russo, V.; Bonelli, B.; Di Serio, M.; Silvestri, B.; Vergara, A.; Aronne, A. A sol-gel ruthenium–Niobium–silicon mixed-oxide bifunctional catalyst for the hydrogenation of levulinic acid in the aqueous phase. *ChemCatChem* **2017**, *9*, 1476–1486. [CrossRef]
41. Rossetti, I.; Bonelli, B.; Ramis, G.; Bahadori, E.; Nasi, R.; Aronne, A.; Esposito, S. New insights into the role of the synthesis procedure on the performance of Co-based catalysts for ethanol steam reforming. *Top. Catal.* **2018**, *61*, 1734–1745. [CrossRef]
42. Farsad, A.; Ahmadpour, A.T.R.; Bastami, T.R.; Yaqubzadeh, A. Synthesis of strong silica aerogel by PEDS at ambient conditions for adsorptive removal of para-dichlorobenzene from water. *J. Sol-Gel Sci. Technol.* **2017**, *84*, 246–257. [CrossRef]
43. Vareda, J.P.; Durães, L. Functionalized silica xerogels for adsorption of heavy metals from groundwater and soils. *J. Sol-Gel Sci. Technol.* **2017**, *84*, 400–408. [CrossRef]
44. Garcia-Valcarcel, A.; Tadeo, J. Influence of soil moisture on sorption and degradation of hexazinone and simazine in soil. *J. Agric. Food Chem.* **1999**, *47*, 3895–3900. [CrossRef] [PubMed]
45. Gunasekara, A.S.; Troiano, J.; Goh, K.S.; Tjeerdema, R.S. Chemistry and fate of simazine. *Rev. Environ. Contam. Toxicol.* **2007**, *189*, 1–23. [PubMed]
46. Troiano, J.; Weaver, D.; Marade, J.; Spurlock, F.; Pepple, M.; Nordmark, C.; Bartkowiak, D. Summary of well water sampling in California to detect pesticide residues resulting from non-point sources applications. *J. Environ. Qual.* **2001**, *30*, 448–459. [CrossRef] [PubMed]
47. Hayes, T.; Case, P.; Chui, S.; Chung, D.; Haeffele, C.; Haston, K. Pesticide mixtures, endocrine disruption, and amphibian declines: Are we understing the impact? *Environ. Health Perspect.* **2006**, *1*, 40–50. [CrossRef] [PubMed]
48. McGhee, I.; Sannino, F.; Gianfreda, L.; Burns, R.G. Bioavailability of 2,4-D sorbed to a chlorite-like complex. *Chemosphere* **1999**, *39*, 285–291. [CrossRef]
49. Sannino, F.; Iorio, M.; De Martino, A.; Pucci, M.; Brown, C.D.; Capasso, R. Remediation of waters contaminated with ionic herbicides by sorption on polymerin. *Water Res.* **2008**, *42*, 643–652. [CrossRef]
50. Sannino, F.; Iorio, M.; Addorisio, V.; De Martino, A.; Capasso, R. Comparative study on the sorption capacity of cyhalofop acid on polymerin, and on a ferrihydrite-polymerin complex. *J. Agric. Food Chem.* **2009**, *57*, 5461–5467. [CrossRef] [PubMed]
51. Addorisio, V.; Pirozzi, D.; Esposito, S.; Sannino, F. Decontamination of waters polluted with simazine by sorption on mesoporous metal oxides. *J. Hazard. Mater.* **2011**, *196*, 242–247. [CrossRef] [PubMed]
52. Sannino, F.; Ruocco, S.; Marocco, A.; Esposito, S.; Pansini, M. Cyclic process of simazine removal from waters by adsorption on zeolite H-Y and its regeneration by thermal treatment. *J. Hazard. Mater.* **2012**, *229–230*, 354–360. [CrossRef] [PubMed]
53. Sannino, F.; Ruocco, S.; Marocco, A.; Esposito, S.; Pansini, M. Simazine removal from waters by adsorption on porous silica tailored by the sol-gel technique. *Microporous Mesoporous Mater.* **2013**, *180*, 178–186. [CrossRef]

54. Esposito, S.; Sannino, F.; Pansini, M.; Bonelli, B.; Garrone, E. Modes of interaction of simazine with the surface of model amorphous silica in water. *J. Phys. Chem. C* **2013**, *117*, 11203–11210. [CrossRef]
55. Sannino, F.; Marocco, A.; Garrone, E.; Esposito, S.; Pansini, M. Adsorption of simazine on zeolite H-Y and sol-gel technique manufactured porous silica: A comparative study in model and natural waters. *J. Environ. Sci. Health, Part B* **2015**, *50*, 779–789. [CrossRef]
56. Sannino, F.; Pansini, M.; Marocco, A.; Bonelli, B.; Garrone, E.; Esposito, S. The role of outer surface/inner bulk Brønsted acidic sites in the adsorption of a large basic molecule (simazine) on H-Y zeolite. *Phys. Chem. Chem. Phys.* **2015**, *17*, 28950–28957. [CrossRef]
57. Esposito, S.; Sannino, F.; Armandi, M.; Bonelli, B.; Garrone, E. Modes of interaction of simazine with the surface of amorphous silica in water. Part II: Adsorption at temperatures higher than ambient. *J. Phys. Chem.* **2013**, *117*, 27047–27051. [CrossRef]
58. Pansini, M.; Sannino, F.; Marocco, A.; Allia, P.; Tiberto, P.; Barrera, G.; Polisi, M.; Battista, E.; Netti, P.A.; Esposito, S. Novel process to prepare magnetic metal-ceramic nanocomposites from zeolite precursor and their use as adsorbent of agrochemicals from water. *J. Environ. Chem. Eng.* **2018**, *6*, 527–538. [CrossRef]
59. Dell'Agli, G.; Ferone, C.; Mascolo, G.; Pansini, M. Crystallization of monoclinic zirconia from metastable phase. *Solid State Ion.* **2000**, *127*, 223–230. [CrossRef]
60. Clayden, N.; Esposito, E.; Ferone, C.; Pansini, M. 27Al and 28Si NMR study of the thermal transformation of Ba-exchanged zeolite A into monoclinic celsian. *J. Mater. Chem.* **2003**, *13*, 1681–1685. [CrossRef]
61. Dell'Agli, G.; Mascolo, G.; Mascolo, M.C.; Pagliuca, C. Thermal behaviour and structural modification of hydrous zirconia gel. *J. Am. Ceram. Soc.* **2008**, *91*, 3375–3379. [CrossRef]
62. Schneegurt, M.A.; Jain, G.C.; Menicucci, J.A., Jr.; Brown, S.A.; Kemner, K.M.; Garofalo, D.F.; Quallick, M.R.; Neal, C.R.; Kulpa, C.F., Jr. Biomass products for the remediation system. *Commun. Agric. Appl. Biol. Sci.* **2001**, *69*, 712–732.
63. Capasso, R.; De Martino, A.; Arienzo, M. Recovery and characterization of the metal polymeric organic fraction (polymerin) from olive oil waste wasters. *J. Agric. Food Chem.* **2002**, *50*, 5170–5176. [CrossRef] [PubMed]
64. European Commission Directive 2002/64/EC of July 18, 2002 concerning the inclusion of cyhalofop-butyl in Annex I to Directive 91/414/EEC. *Off. J. L* **2002**, *189*, 0027–0032.
65. Giles, C.H.; Smith, D.; Huitson, A. A general treatment and classification of the solute adsorption isotherms. *I Theoretical. J. Colloid Interface Sci.* **1974**, *47*, 755–765. [CrossRef]
66. Esposito, S.; Garrone, E.; Marocco, A.; Pansini, M.; Martinelli, P.; Sannino, F. Application of highly porous materials for simazine removal from aqueous solution. *Environ. Technol.* **2016**, *37*, 2428–2434. [CrossRef]
67. Baerlocher, C.; Meier, W.M.; Olson, D.H. *Atlas of Zeolite Framework Types*; Elsevier: Amsterdam, The Netherlands, 2001; pp. 132–133.
68. Breck, D.W. *Zeolite Molecular Sieves: Structure, Chemistry and Use*; Wiley: New York, NY, USA, 1974.
69. Marocco, A.; Dell'Agli, G.; Spiridigliozzi, L.; Esposito, S.; Pansini, M. The multifarious aspects of the thermal conversion of Ba-exchanged zeolite A to monoclinic celsian. *Microporous Mesoporous Mater.* **2018**, *256*, 235–250. [CrossRef]
70. Sannino, A.; Violante, L.; Gianfreda, L. Adsorption-desorption of 2,4-D by hydroxi aluminium montmorillonite complexes. *Pestic. Sci.* **1997**, *51*, 429–435. [CrossRef]
71. Violante, A.; Ricciardella, M.; Pigna, M. Adsorption of heavy metals on mixed Al-Fe oxides in tha absence or presence of organic ligands. *Water Air Soil Poll.* **2003**, *145*, 289–306. [CrossRef]
72. Rouquerol, F.; Rouquerol, J.; Sing, K. *Adsorption by Powders and Porous Solids: Principles, Methodology, and Application*; Academic Press: London, UK, 1999.
73. Esposito, S.; Marocco, A.; Bonelli, B.; Pansini, M. Produzione di materiali compositi metallo-ceramici nano strutturati da precursori zeolitici. *Italian Patent n. MI* **2014**, *A*, 000522.
74. Esposito, S.; Marocco, A.; Bonelli, B.; Pansini, M. Production of Magnetic Metal Nanoparticles Embedded in a Silica-Alumina Matrix. U.S. Patent Application 15/128,301; PCT International Application Published under Number WO 2015/145230 A1, 21 June 2018.
75. Ronchetti, S.; Turcato, E.A.; Delmastro, A.; Esposito, S.; Ferone, C.; Pansini, M.; Onida, B.; Mazza, D. Study of the thermal transformations of Co- and Fe-exchanged zeolites A and X by"in situ" XRD under reducing atmosphere. *Mater. Res. Bull.* **2010**, *45*, 744–750. [CrossRef]

76. Marocco, A.; Dell'Agli, G.; Esposito, S.; Pansini, M. Metal-ceramic composite materials from zeolite precursor. *Solid State Sci.* **2012**, *14*, 394–400. [CrossRef]
77. Esposito, S.; Dell'Agli, G.; Marocco, A.; Bonelli, B.; Allia, P.; Tiberto, P.; Barrera, G.; Manzoli, M.; Arletti, R.; Pansini, M. Magnetic metal-ceramic nanocomposites obtained from cation-exchanged zeolite by heat treatment in reducing atmosphere. *Microporous Mesoporous Mater.* **2018**, *268*, 131–143. [CrossRef]
78. Barrera, G.; Tiberto, P.; Esposito, S.; Marocco, A.; Bonelli, B.; Pansini, M.; Manzoli, M.; Allia, P. Magnetic clustering of Ni^{2+} ions in metal-ceramic nanocomposites obtained from Ni-exchanged zeolite precursors. *Ceram. Int.* **2018**, *44*, 17240–17250. [CrossRef]
79. Barrera, G.; Tiberto, P.; Allia, P.; Bonelli, B.; Esposito, S.; Marocco, A.; Pansini, M.; Leterrier, Y. Magnetic properties of nanocomposites. *Appl. Sci.* **2019**, *9*, 212. [CrossRef]
80. Barrera, G.; Allia, P.; Bonelli, B.; Esposito, S.; Freyria, F.S.; Pansini, M.; Marocco, A.; Confalonieri, G.; Arletti, R.; Tiberto, P. Magnetic behavior of Ni nanoparticles and Ni^{2+} ions in weakly loaded zeolitic structures. *J. Alloys Compd.* **2019**, *817*. [CrossRef]
81. Pansini, M.; Dell'Agli, G.; Marocco, A.; Netti, P.A.; Battista, E.; Lettera, V.; Vergara, P.; Allia, P.; Bonelli, B.; Tiberto, P.; et al. Preparation and Characterization of Magnetic and Porous Metal-Ceramic Nanocomposites from a Zeolite Precursor and Their Application for DNA Separation. *J. Biomed. Nanotechnol.* **2017**, *13*, 337–348. [CrossRef]
82. Weidentaler, C.; Zibrovius, B.; Schimanke, J.; Mao, Y.; Mienert, B.; Bill, E.; Schmidt, W. Oxidation behaviour of ferrous cations during ion exchange into zeolites under atmospheric conditions. *Microporous Mesoporous. Mater.* **2005**, *84*, 302–317. [CrossRef]
83. Gualtieri, A.F.; Mazzucato, E.; Venturelli, P.; Viani, A.; Zannini, P.; Petras, L. X-ray powder diffraction quantitative analysis performed in situ at high temperature: Application to the determination of NiO in ceramic pigments. *J. Appl. Crystallogr.* **1999**, *32*, 808–813. [CrossRef]
84. Larson, A.C.; Von Dreele, R.B. *General Structure Analysis System "GSAS"*; Los Alamos National Laboratory Report LAUR 86-748; Los Almos National Laboratory: Los Almos, NM, USA, 1994.
85. Toby, B.H. EXPGUI, a Graphical User Interface for GSAS. *J. Appl. Crystallogr.* **2001**, *34*, 210–213. [CrossRef]
86. Wilson, J.L.; Poddar, P.; Frey, N.A.; Srikant, H.; Mohomed, K.; Harmon, J.P.; Kotha, S.; Wachsmith, J. Synthesis and magnetic properties of polymer nanocomposites with embedded iron nanoparticles. *J. Appl. Phys.* **2004**, *95*, 1439–1443. [CrossRef]
87. Bhaumik, M.; Choi, H.J.; McCrindle, R.I.; Moity, A. Composite nanofibers prepared from metallic iron nanoparticles and polyaniline: High performance for water treatment applications. *J. Colloid Interface Sci.* **2014**, *425*, 75–82. [CrossRef] [PubMed]
88. Melzak, K.A.; Sherwood, C.S.; Turner, R.F.B.; Haynes, C.A. Driving Forces for DNA adsorption to silica in perchlorate solution. *J. Colloid Interface Sci.* **1996**, *181*, 635–644. [CrossRef]
89. Li, X.; Zhang, J.; Gu, H. Adsorption and desorption behaviors of DNA with magnetic mesoporous nanoparticles. *Langmuir* **2011**, *27*, 6099–6106. [CrossRef]
90. Xu, P.; Zeng, G.M.; Huang, D.L.; Hu, S.; Zhao, M.H.; Lai, C.; Wei, Z.; Huang, C.; Xie, G.X.; Lin, Z.F. Use of iron oxide nanomaterials in wastewater treatment: A review. *Sci. Total Environ.* **2012**, *424*, 1–10. [CrossRef]
91. Abdel Maksoud, M.I.A.; Elgarahy, A.M.; Farrell, C.; Al-Muhtaseb, A.H.; Rooney, D.W.; Osman, A.I. Insight on water remediation application using magnetic nanomaterials and biosorbents. *Coord. Chem. Rev.* **2020**, *403*, 213096. [CrossRef]